"THE ACTION OF A SOUND FIELD ON COLLOIDS"

A thesis presented for the
degree of Master of Science in Physics
in the University of Canterbury,
Christchurch, New Zealand.

by

D. J. Lockwood

1964

CONTENTS

ACKNOWLEDGMENTS

I wish to thank the Physics Department of the University of Canterbury for the opportunity to carry out this research.

I am particularly grateful to my supervisor, Dr. T. J. Seed, for his guidance and kindly interest in the research work .

My thanks to Mr. C. J. Wornall for his theoretical and practical help in the electronic projects; to Mr. E. R. Mangin for the photographic reproductions; to the Mechanical Workshop staff for their considerable help in the mechanical constructions; and to Mr. R. P. Borrall for constructing the Photomultiplier Photometer.

SUMMARY

The effect of high frequency sound waves on colloids is investigated experimentally by observing the behaviour of the pattern produced by the diffraction of light by progressive ultrasonic waves. The results show that disc- and needle-shaped colloids are affected by the ultrasonic waves, producing variations in the diffraction pattern.

A complete description of the apparatus is given, together with the chemical preparations and the experimental methods used.

CHAPTER 1

INTRODUCTION

This research was the result of a desire to obtain further knowledge of clays and, in particular, clay-water systems. At the present time the physical behaviour of clays is uncertain. Projects in which clay is used, such as dam and road construction, well drilling, brick and pottery making, and even hydrometer soil analysis, rely either on calculations based on false assumptions or on the testing of samples and scale models for their success.

The calculations on clay behaviour are based on the supposition that clays consist of approximately spherical particles, for which the theory is well known. Evidence that this assumption is not true has been given by electron micrographs of clays. It has been found that the three main types of clay have a particle shape thus,

Clay type	Particle shape
the Halloysites	elongated needles
the Kaolinites	hexagonal plates
the Montmorillonites	sheet-like, but no definite structure

(A typical particle size would be 10^{-4} cm (1μ) for the largest dimension and 10^{-7} cm (10Å) for the smallest dimension.) This appearance can be explained on the principle of their elemental structure.

Clays have the property of absorbing water in between layers of the clay structure and thus, even though the clay may appear to be solid, some water may be present due to this absorption. Thus clays are, in effect, clay-water systems. Furthermore, in clay-water systems the clay is in the colloidal state.

Colloids

A definition: "The property which characterizes the colloidal state is the size of those units which can be considered as independent in the structure."

These units or suspended particles may range in size from 1 mμ (10Å) to 5μ (50,000Å) though these limits are arbitrary.

Colloids may be classified into systems as follows,

Finely Divided Part (the colloidal particle)	Continuous Part (the dispersing material)	Type of Colloid
Gaseous	Gaseous	None (complete mixing of gases)
Liquid	Gaseous	Fog
Solid	Gaseous	Smoke
Gaseous	Liquid	Foam
Liquid	Liquid	Emulsion
Solid	Liquid	Sols, gels, pastes [a]
Gaseous	Solid	Solid foam
Liquid	Solid	Solid sol
Solid	Solid	Solid sol

[a] The amount of liquid present determines whether a colloid is a sol, gel or paste.

Clay-water systems are thus classified as sols.

Sols

There are three main types of sol which have the properties listed below.

Type of Sol	Main Properties	Examples
Lyophobic sols	Normally no attraction between the particles and the liquid	Gold sol (small gold particles in water)
Lyophilic sols	Strong attraction between the particles and the liquid (particles are often molecules of colloidal size)	Introcellulose in acetone, polystyrene in toluene
Colloidal electrolytes	Exhibit properties of both colloids and electrolytes in aqueous solution. (One can describe this behaviour as a substitution of one of the ions of the electrolyte by charged colloidal particles.)	Soaps, dyes and detergents

As clays are predominantly lyophobic in nature, we will consider lyophobic sols further.

Lyophobic Sols

The density of the colloidal particles in lyophobic sols is usually greater than that of the liquid. Thus the particles would eventually settle out of solution due to the effect of gravity if it were not for several opposing factors. These factors are (a) a partial opposition by viscous resistance, (b) the circulating action of small convection currents and (c) the Brownian motion of the suspended particles. Factor (c) has the greatest effect, especially in the case of small particles. For example, consider silver spheres of various sizes.

Diameter of sphere	Distance moved in one second due to	
	Brownian	Gravitational Motion
0.1 μ	10 μ	0.07 μ
1 μ	3 μ	7 μ
10 μ	1 μ	700 μ

Hence a sol will be stable if the suspended particles are sufficiently small. For this reason linking of particles cannot take place to any extent.

Normally, linking would take place due to the random nature of Brownian motion which would bring particles close enough so that the short-range Van der Waals forces could act. In lyophobic sols this linking is prevented by the repulsive action of a screen of similar electric charges that surrounds each particle. This charge is acquired either by ionisation

or, more commonly, by absorption of ions at the particle surface. This point of view is confirmed by the fact that stable sols are not normally produced except in the presence of ions.

Particles in lyophobic sols are generally spherical in shape (e.g., red gold, sulphur, arsenious sulphide and fine silver sols), though some are plate-like (e.g., blue gold and aged hydrous ferric oxide) and some needle-like (e.g., aged vanadium pentoxide). These shapes have been verified by "Streaming Double Refraction" experiments.[1]

As it is simpler to synthesise these colloids of known shape than to use clay samples of doubtful shape, the initial investigations will be carried out on lyophobic sols of similar particle shape to that of clays.

Ultrasonic Waves

The original intention of this research was to investigate the action of high frequency sound waves on colloidal particles that are similar in shape to clays. And possibly provide some practical information on the compacting and forming of clays as a result.

It was expected that the sound waves travelling through the suspending medium would align the needle- and disc-shaped particles in preferred directions. This idea is supported by the fact that double refraction experiments have shown that

flows orientate anisometric colloidal particles.

Streaming Double Refraction

Streaming double refraction occurs in certain colloidal solutions when they are stirred or allowed to stream or flow through a tube. On examination between crossed polaroids, the field lights up and stream lines appear on account of the scattering and repolarisation of the incident polarised light. Such sols must contain particles that are orientated by flow. Hence they are rod-like or disc-shaped, but not spherical.[2] It is found that rods will place themselves parallel with the stream lines whereas discs place themselves at right angles except near the wall of the tube where they will tend to be parallel with the longest axis in the direction of flow.[3]

Alignment of the Colloidal Particles

While searching the literature for information on streaming double refraction, I found four papers on the topic of this thesis.

In 1938, H. Kawamura observed that under the action of ultrasonic waves a vanadium pentoxide sol became doubly refracting.[4] Further, Bömmel and Nikitine[4] found that if the light traversing the sol is polarised and transmitted in a direction perpendicular to the direction of propagation of the ultrasonic waves, then a set of equidistant fringes is seen through a crossed Nicol. These fringes corresponded to anti-

nodes of the sound waves. S. Oka[5] has formulated a theory to account for these observations.

Oka attributes the double refraction phenomenon to the orientating effect of the sound waves on the aniso-dimensional particles. The particles remain orientated, despite the sinusoidal variation in the sound field, because of their large relaxation time compared with the ultrasonic period.

(No more-recent papers were found on this subject.)

It was originally intended to observe the orientation of colloidal particles by their effect on the diffraction pattern which is obtained when collimated light is passed at right angles through a sound wave. Although the expected orientation has been observed, its effect on the diffraction pattern does not appear to have been investigated. And this has become the purpose of this research: "To investigate the effect of clay-type colloids on the diffraction of light by ultrasonic waves in liquids." A secondary aim is: "To verify that the orientation of the colloidal particles does take place."

Diffraction of Light by Ultrasonic Waves

This effect was first observed by Debye and Sears in 1932.[6]

Parallel light is passed through a plane progressive (or stationary) sound wave travelling in a liquid and is then

focussed on a screen to produce the diffraction pattern. (The width of the light beam must be greater than the wavelength of sound in the liquid for the diffraction pattern to appear. For megacycle per second sound waves this condition is easily achieved.) Figure 1 shows this in diagramatic form. S is the light source; lens L_1 focusses S onto slit SL; the light is collimated by lens L_2, and, after passing through the sinusoidal progressive sound wave, is focussed by lens L_3 onto the screen.

Debye and Sears found that the spacing of the orders depended on both the light frequency and the sound frequency, and that the number of orders visible depended on the intensity of the sound wave.

A theory explaining these effects has been proposed by Raman and Nath.[7] The plane ultrasonic wave produces a periodic variation in the index of refraction of the liquid. The light passing through the liquid will be retarded in phase, the amount of retardation depending upon which portion of the ultrasonic wave it passes through. This results in the emerging light front being modulated in phase, and it is this phase modulation that produces the diffraction pattern. The light intensity distribution in the diffraction pattern is determined by the form of the phase modulation.[8]

For a sine-wave modulation, the Raman and Nath theory gives the relationship

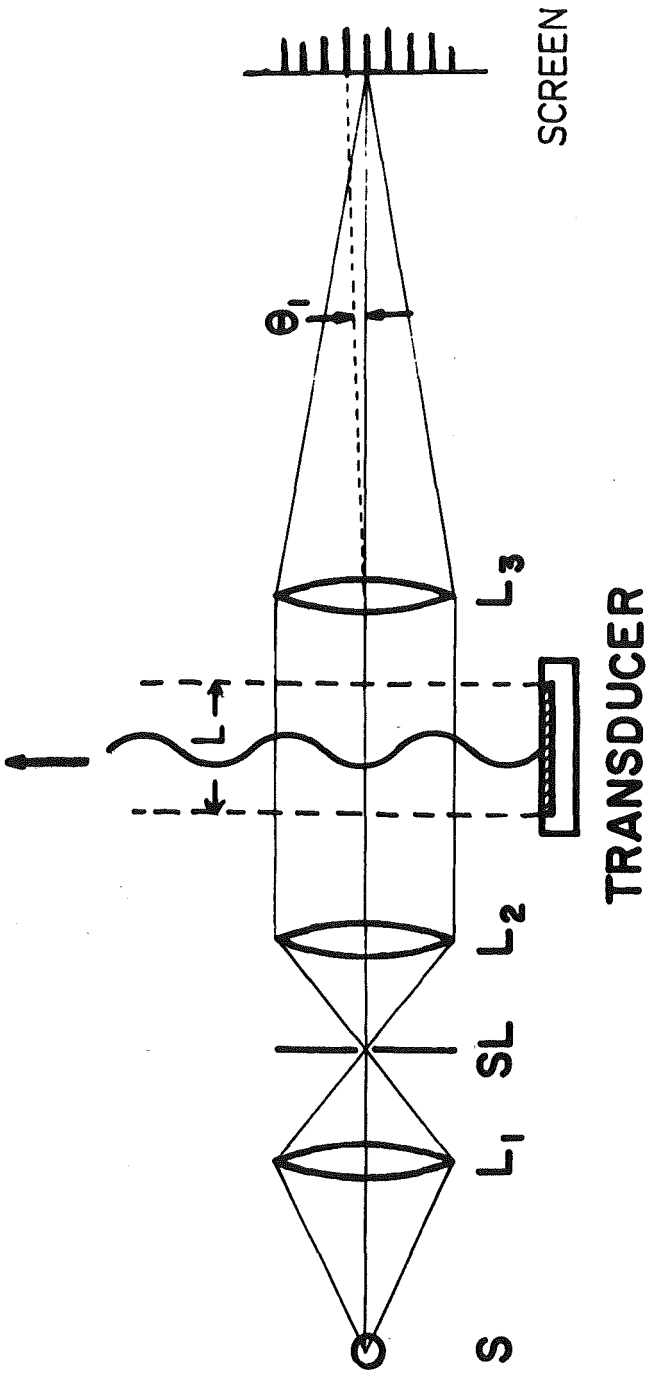

Figure 1

Optical arrangement for observing the diffraction of light.

$\text{Sin}\ \theta_n = -\frac{n\lambda}{\lambda^*}$ for the variation in the spacing of orders with frequency where θ_n is the angle of the n^{th} order of the diffraction pattern (see Fig. 1).

λ is the wavelength of the light.

λ^* is the wavelength of the sound.

n is any integer, positive, negative or zero. (n=o corresponds to the central undiffracted line of the diffraction pattern.)

and the intensity of the n^{th} order is given by

$$I_{+n} = I_{-n} = J_n^2 (V_\phi)$$

where J_n = the n^{th} order Bessel Function

and $V_\phi = V_o \text{Sec}\,\phi \left[\frac{\text{Sin}X}{X}\right]$

where $X = \frac{\pi L}{\lambda^*} \text{Tan}\,\phi$

ϕ is the angle of incidence of the light beam, measured from normal incidence

L is the width of the ultrasonic beam

V_o is the Raman-Nath parameter for normal incidence and is given by

$$V_o = \frac{2\pi \Delta\mu L}{\lambda}$$

where $\Delta\mu$ is the maximum change produced by the ultrasonic wave in the index of refraction of the liquid.

Hence the intensity of the orders, and the number of orders visible, depends upon the driving amplitude of the transducer as this is proportional to $\Delta\mu$. Hence the actual

voltage across the transducer, which is proportional to the amplitude of the ultrasonic wave produced, is proportional to the Raman-Nath parameter V_o.

There is also a Doppler effect associated with the diffraction pattern such that

$$f_m = f_L \pm mf_S$$

where f_m is the frequency of the light in the m^{th} order.

f_L is the frequency of the incident light.

f_S is the frequency of the sound wave.

m is an integer.

This effect has been observed recently by Cummins, Knalde, Grampel and Yeh.[9]

Mayer[10] has shown that the Raman-Nath theory holds very well for low sound intensities (as there is little finite amplitude distortion of the sinusoidal sound wave[8]) and for sound frequencies less than an arbitrary 8 Mc/sec.

Figures 2 and 3 depict typical Raman-Nath diffraction spectra. Fig. 2 (reproduced from a paper by Breazeale and Hiedemann[11]) shows how the intensity of the sound wave affects the diffraction pattern. Fig. 3 (reproduced from a paper by Mayer[10]) shows the effect of varying the angle of incidence.

When sound frequencies are high (greater than the arbitrary 8 Mc/sec) and the sound beam is wide, an effect

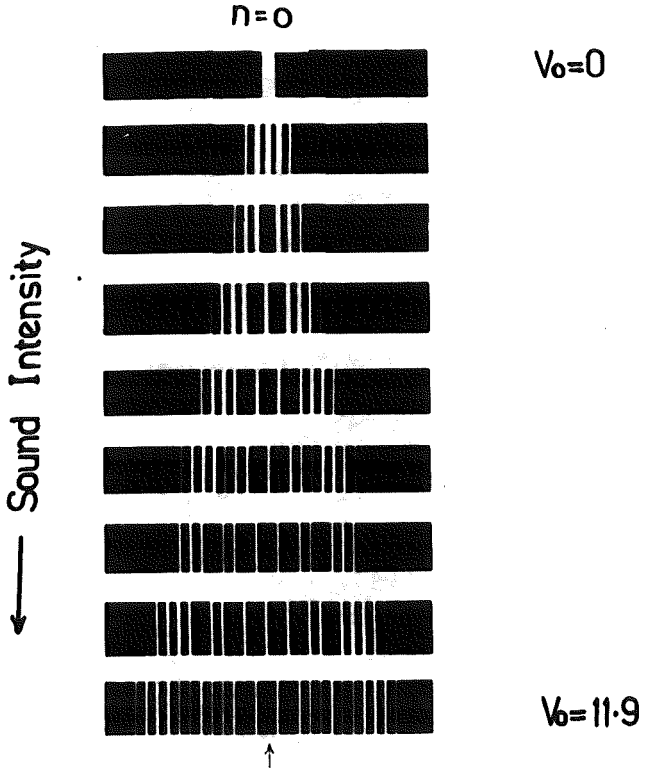

FIG.2 Light diffraction by ultrasonic waves in water. (Diffraction pattern as a function of sound intensity.)

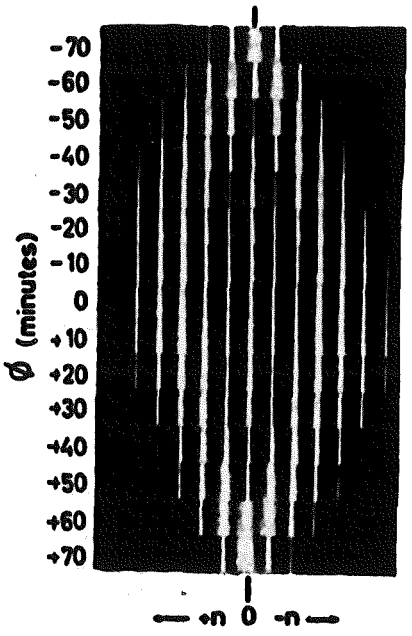

FIG.3 Light diffraction by ultrasonic waves in water. (Diffraction pattern as a function of angle of incidence.)

similar to Bragg X-ray reflection in crystals is apparent, and positions of maximum intensity of the diffracted light are given by

$$p\lambda = 2\lambda^* \text{ Sin}$$

where p is an integer.

David[10] has modified the Raman-Nath equations to allow for this, giving

$$I_{\pm 1} = \left[\tfrac{1}{2}V_o \left(\frac{\text{Sin } Y}{Y}\right)\right]^2$$ for the intensity of the first order.

where $$Y = \frac{\pi L}{\lambda^*}\left(\phi \pm \frac{\lambda}{2\lambda^*}\right)$$

At the higher frequencies, a diffraction pattern is obtained (as in the Raman-Nath theory) but high intensity in a given portion of the spectrum is obtained only when the $p\lambda = 2\lambda^* \sin\phi$ Bragg relation holds. At considerably higher frequencies (around 20 Mc/sec) the Bragg effect predominates.

Hence, given suitable conditions, the behaviour of the diffraction pattern is predictable and thus any differences produced in the pattern by the orientation of colloidal particles would be seen. The expected behaviour is that a pronounced Bragg effect will be observed at lower than normal frequencies, as well as a non-normal distribution of the intensities of the various orders. This is particularly so in the case of plate-like colloids where the alignment is

perpendicular to the direction of flow (i.e., the direction of propagation of the ultrasonic wave).

CHAPTER 2

PRODUCTION OF THE SOUND WAVES

The Ultrasonic Tank

The Debye-Sears phenomenon utilises plane progressive sound waves of high frequency. The study of progressive ultrasonic waves in liquids requires a tank that will contain the liquid and give true progressive waves in the region of interest. The ultrasonic tank outlined in Figure 4 was designed to meet these specifications.

The curved walls of the lining guide the sound waves away from the windows--the region of interest. The outer arc was originally designed to be the Pedal curve of the inner arc, but it has been approximated to a segment of a circle for ease of construction. (The error involved in this approximation is small, about 1%.)

By taking the angle of incidence equal to the angle of reflection, geometrical constructions on paper show that the sound waves bounce from wall to wall at least fourteen times before returning to the region of interest. It is required to line the tank with an absorber so that the returning sound waves will be attenuated to insignificant proportions. (All tank designs yet seen seem to rely on this factor for their successful (?) operation.) Typical attenuating materials that have been used previously are castor oil (separated from the

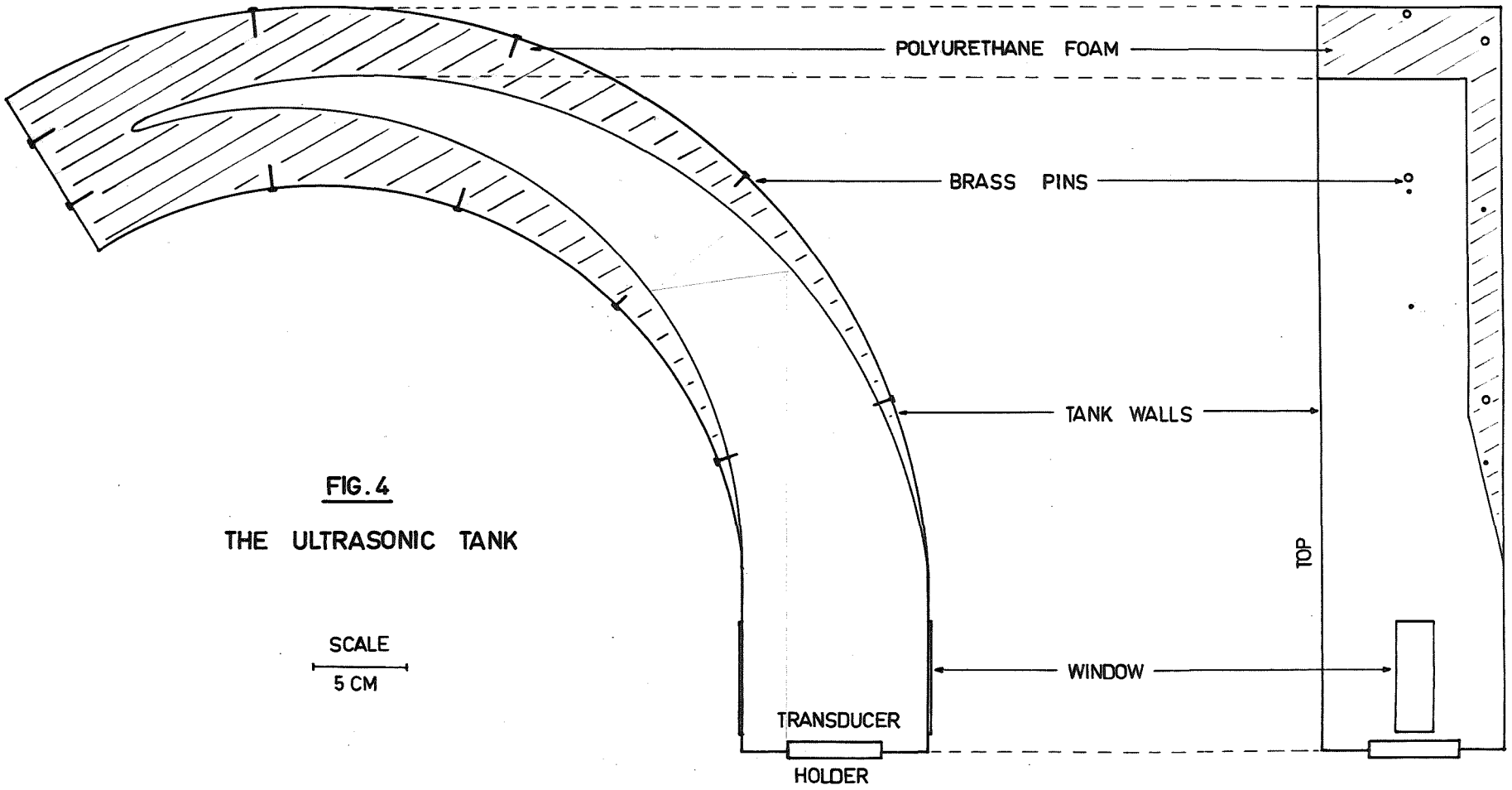

FIG. 4

THE ULTRASONIC TANK

tank proper by thin membranes), cork and steel wool linings.

The present tank design requires an absorbing material that can be moulded to shape and will retain that shape. A polyurethane foam (trade name "Solite") was chosen as the absorbing material. A resin and a hardener are mixed together in liquid form; the mixture foams and then sets hard. By volume, 90% of the foam consists of air cells whose size depends on the temperature at which they were formed--the higher the temperature, the larger the cells. (At room temperature, the cells have an average diameter of 0.4 mm.)

Because of the high percentage of air cells the density of the foam material is much less than that of water, and thus its acoustic impedance is less than that of water. Hence, with water in the tank, there would be a bad mismatch of impedances at the interface between the water and the foam lining. This would have the effect of reflecting most of the sound incident on this interface (i.e., absorption would be poor). However, three factors counteract this,

(1) the foam absorbs water over a period of time (several days), which would help to bring about a closer impedance match.

(2) the wavelength of sound in water is 0.3 mm approximately for a frequency of 5 Mc/sec. Thus a hole size of 0.4 mm is significant at megacycle frequencies and the foam does not present the smooth surface that would be apparent

at longer wavelengths. The holes will have the effect of diffusely scattering the incident sound waves and thus break up the strong reflections, as well as assisting the sound to penetrate the foam.

(3) the gradually narrowing tank provides an artificial acoustic impedance match between the liquid and the foam lining so that increased absorption should result as the sound waves progress further into the tank.

Tank Construction

The tank sides were cut out of 1/32 inch brass sheet and rolled to shape. The sides were sweat soldered to a heavy plate base ($\frac{1}{8}$ inch brass).

The tank lining was made by first constructing a mould in the desired shape. The foaming mixture was then poured around the mould and, when set, the mould was removed. The glossy finish produced by the mould was removed by filing with a coarse rasp. (This filing had the desirable side effect of considerably roughening the surface of the lining.) Brass pins, shown in Fig. 4, were used to hold the lining in place.

The tank windows manufactured from glass photographic slide-covers, were fastened in place with Pliobond cement.

A drain plug was fitted so that the tank could be emptied easily.

The completed tank was bolted to a "Handy-Angle" steel frame to prevent accidental movement of the tank.

The Transducer

The production of a plane wave requires that the following dimension conditions hold.[12]

$$l, b > 10\lambda$$

$$d > \lambda$$

where l = length of tank

b = breadth of tank

d = diameter of transducer

λ = wavelength of sound in the medium
(= 0.3 mm at 5 Mc/sec in water)

Hence the tank size was determined at a 10x10 cm cross-section with a region of interest of 10 cm length. (Here $l, b \approx 300\lambda$.) A transducer diameter of 2.54 cm would be more than adequate. (Here $d \approx 80\lambda$.)

At megacycle frequencies the most commonly used transducer materials are quartz, barium titanate ceramic and PZT (lead zirconate titanate) ceramic. The transducer would be operating in the plate thickness mode and thus in the case of quartz an "X-cut" would be used. The signal voltage is applied across the thickness dimension of the quartz plate, and because of the piezoelectric effect the quartz expands or contracts in the thickness dimension depending on the polarity of the signal voltage. The mechanical motion produces the sound wave. In the case of the ceramics, however, the piezoelectric effect is lost due to the random orientation of the

tiny crystals forming the ceramic. These materials operate on a second order effect, the electrostrictive effect, which is introduced by polarising the ceramic. This permanent polarisation is obtained by applying a D.C. field (of the order of kV's/cm) in the required direction which, in the case of the plate thickness mode, is the thickness direction.

As long term stability is not required the ceramic materials have advantages over quartz. The ceramics possess a much higher dielectric constant requiring a much lower electric field strength for an equal power output from identical radiating areas.

Of the ceramics, PZT has advantages over barium titanate.[13] PZT has

(1) a low dielectric loss so that internal heating is kept to a minimum.

(2) a higher electromechanical coupling factor and therefore gives a greater sound output for equal input (electrical) powers than barium titanate would.

(3) its properties are stable over a wider range of temperature.

(4) ageing effects are negligible.

PZT was thus chosen as the transducer material and was purchased from the Brush Crystal Co. under the following specifications,

Material	PZT-4 (Brush Crystal trade name for a modified PZT ceramic which is suitable for power applications).
Shape	Disc of diameter 2.54 cm, thickness 0.38 mm.
Mode of Vibration	Thickness (therefore polarised in the thickness direction).

The thickness dimension of 0.38 mm corresponds to a natural series resonant frequency of 5 Mc/sec. This frequency was chosen because it enables the Debye-Sears effect to be observed with a minimum amount of Bragg reflection present. However, the Bragg effect can be observed if necessary by operating the transducer at its third harmonic (approximately 15 Mc/sec).

The Transducer Holder

The transducer was mounted in a brass holder constructed to the design shown in Figure 5. (This holder is similar to one described by Noltingk.[14]) The transducer is held in place with Pliobond cement, which serves the double purpose of sealing the transducer in the holder and providing a "flexible" mounting. (Another advantage is that the transducer can be removed from the holder if necessary, whereas in Noltingk's version the transducer is permanently sealed in position with Araldite cement.)

The holder itself forms one electrical contact where the silvered transducer surface touches the holder. The other contact is made to the centre of the other side of the

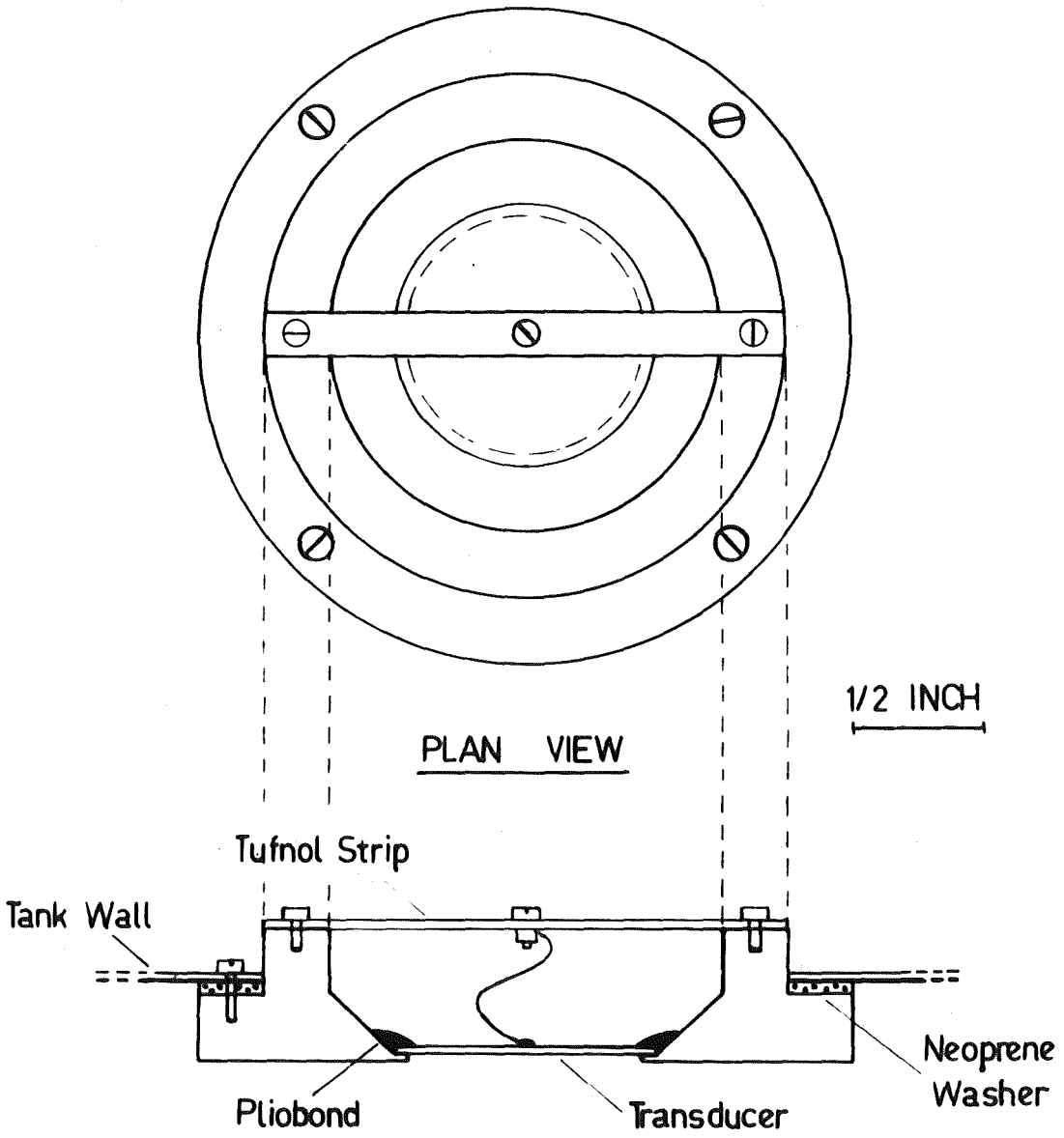

FIG. 5

THE TRANSDUCER HOLDER

transducer, a loop of 5 amp fuse wire being puddle-soldered directly to the surface.

The transducer is air-backed to increase the power radiated into the liquid. The air-transducer interface acts as an almost perfect reflector of the sound waves generated by the transducer, because of the very low acoustic impedance of air these reflected waves are returned in phase with the transducer motion, thereby doubling the amplitude of the radiated wave (i.e., increasing the radiated power to four times the original amount).

A neoprene washer smeared with silicone grease forms the seal between the holder and the tank. Pressure on the seal being maintained by four screws passing through the tank wall into the holder.

The Transducer Power Supply

The maximum electrical power dissipation of PZT-4 is approximately 15 watts/cm^2. [15] For the transducer chosen, which has an electroded area of 5 square cm, the maximum power that can be dissipated is approximately 75 watts, i.e., this is the maximum input power to the transducer. Hence the power supply requirements are 75 watts of R.F. (radio frequency) power at a frequency of 5.0 ± 0.5 Mc/sec with reasonable frequency stability and a sinusoidal waveform.

The circuit shown in Figure 6 was designed to meet these

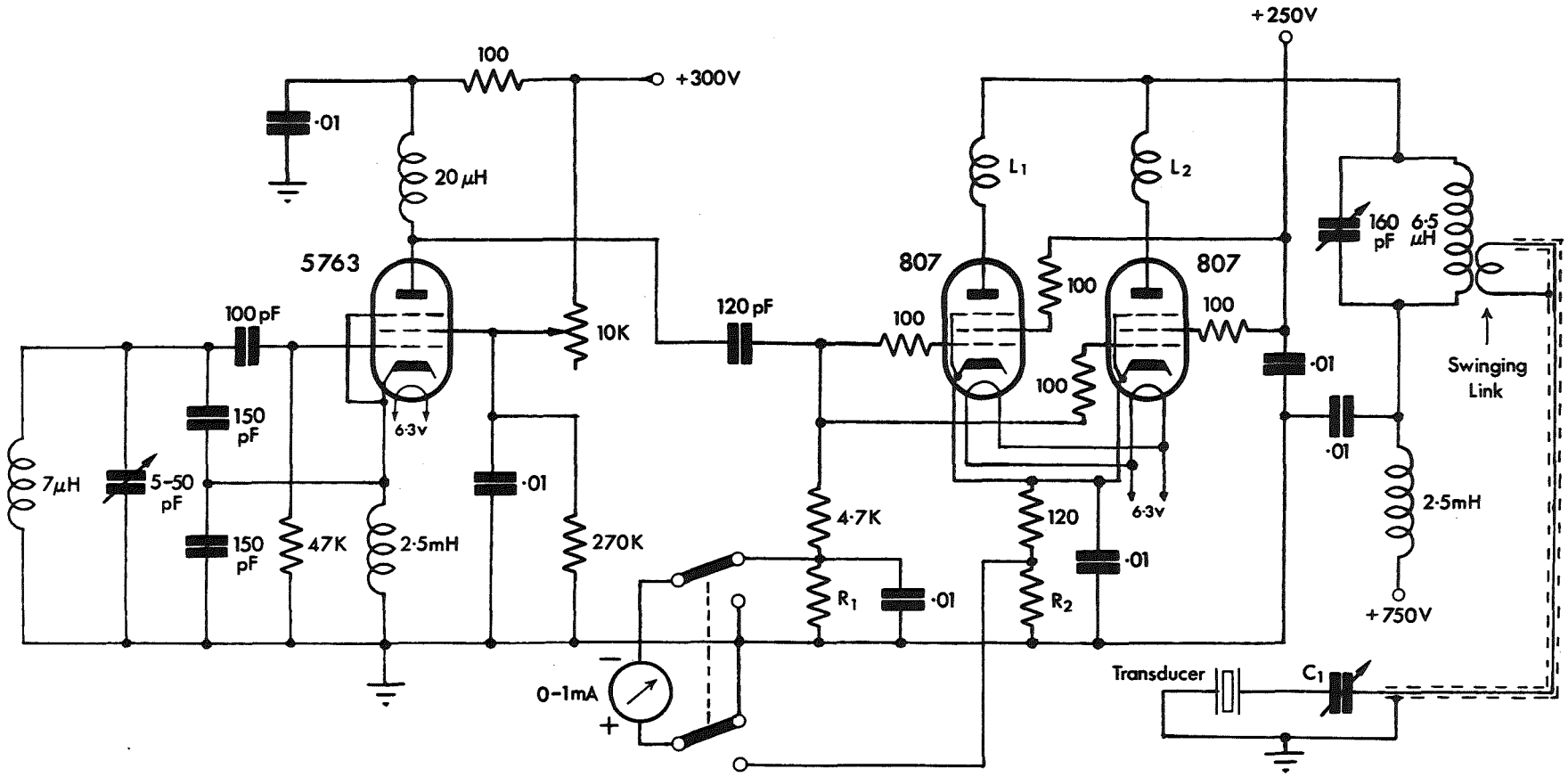

FIG. 6

Circuit of the R. F. Power Supply

specifications.

Circuit description:

The 5763 pentode valve acts as an electron-coupled oscillator. The oscillator section is a Colpitts oscillator which has the advantage of variable tuning with a reasonable frequency stability. The potentiometer in the screen supply of the 5763 acts as a gain control.

The output from this valve drives the Class C power amplifier stage which consists of two 807 beam tetrodes in parallel. This combination produces 100 watts of R.F. power, which is sufficient allowing for losses in the output tank and coupling circuits.

Inductances L_1, L_2 (see Fig. 6) are R.F. chokes consisting of 15 turns of heavy gauge, enamelled wire. L_1 and L_2 in conjunction with the 100 ohm grid and screen stoppers suppress parasitic oscillations.

The meter monitors either the grid drive or the cathode current of the 807's. Resistors R_1 and R_2 are meter shunts that are of such a value that the meter can read either from 0-10 mA or from 0-300 mA depending on the position of the double-pole double-throw switch.

Variable capacitor C_1 enables any inductive reactance in the link circuit to be tuned out thus making the transmitter load purely resistive. (In which case the tuning of the 807 tank circuit will not be affected when the link is

dipped in or out.)

The swinging link enables the amount of power fed to the transducer to be finely and continuously controlled. The link is integral with the tank coil which consists of twelve turns, a gap, then two turns of $\frac{1}{8}$ inch copper tube. The three-turn link dips into the gap left in the "cold" end of the tank coil.

The D. C. Supply

The D.C. (direct current) requirements of the 5763 and the 807's are

+750V at 200 mA

+300V at 100 mA

+250V at 20 mA

A D.C. power supply unit was designed to satisfy these requirements. The circuit of the supply is shown in Figure 7.

Circuit description:

The supply has interlocks to prevent damage in the event of accidents, break-down in components or a temporary break in the mains supply.

The switches facilitate setting up the R.F. supply circuits. Switch S_1 supplies power to the filaments of all valves. S_2 applies high tension to the oscillator section of the R.F. supply only; thus the oscillator can be set to frequency and the grid drive on the 807's adjusted before applying high tension to the 807's by means of switch S_3.

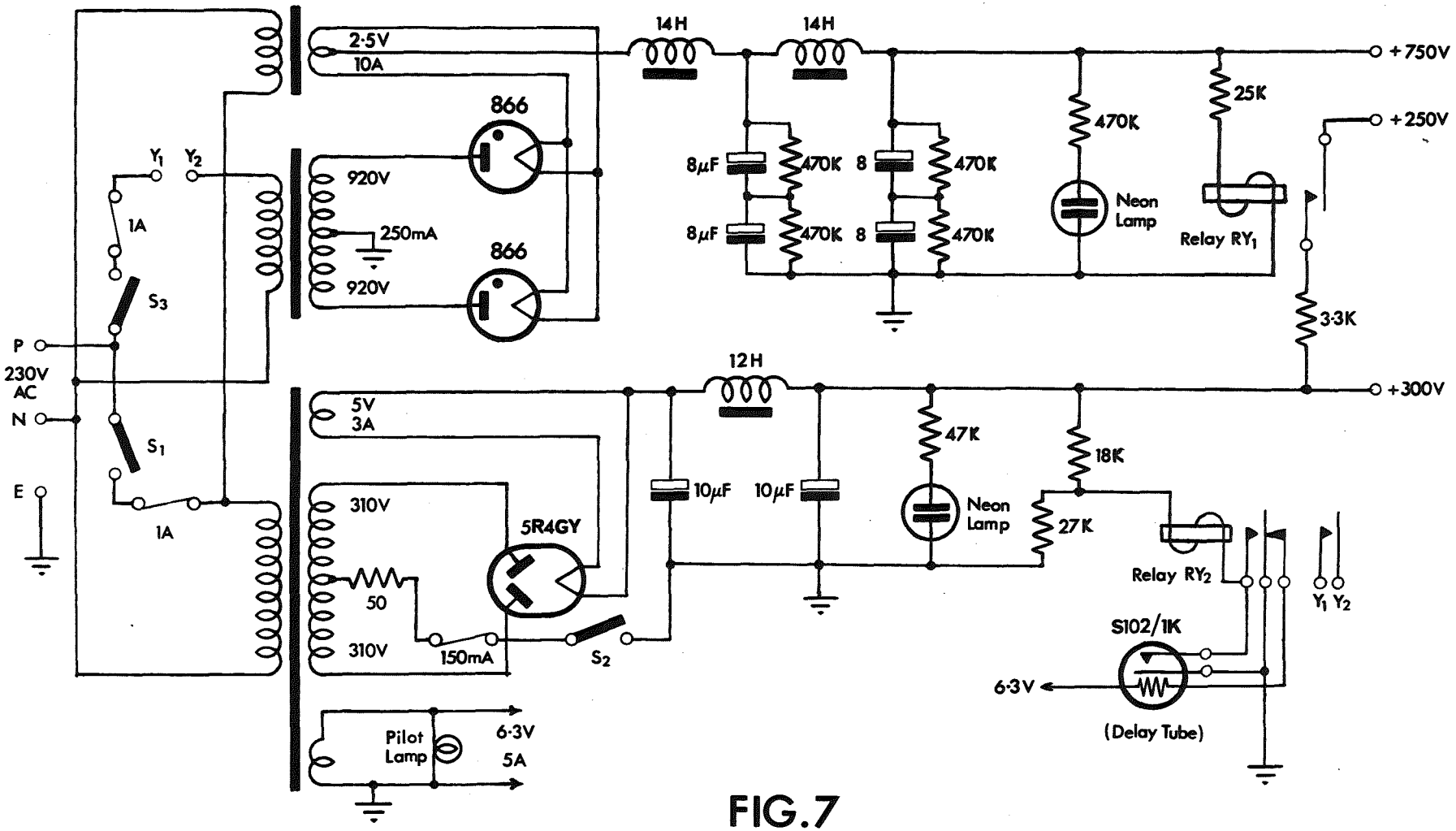

FIG.7

Circuit of the Power Supply Unit

Switches S_1, S_2 and S_3 are normally switched on in the sequence listed, but this is not necessary as the interlocks provide for the correct sequence automatically.

Relay RY_1 applies the screen volts to the 807's at the same time as the plate volts. If the 750V supply breaks down, the relay drops out and removes the screen volts, thus protecting the 807's.

Relay RY_2 operates in conjunction with the one-minute thermal delay tube. The delay tube is incorporated in the circuit to allow the 866 mercury vapour rectifiers sufficient warm-up time before the high tension is applied. Relay RY_2 has contacts which hold the relay on, and these come into action after the initial activation of the relay when the delay tube contacts close. At the same time the 6.3V supply to the delay tube is cut off (which causes its contacts to re-open) and the contacts Y_1, Y_2 close. Any fault which results in a loss of low tension (+300V) will cause RY_2 to drop out and thus switch off the 750V supply. The circuit is so designed that high tension can not be reapplied to the 866's until the delay tube has again closed and the 300V supply is functioning.

Figures 8 and 9 show photographs of the constructed units.

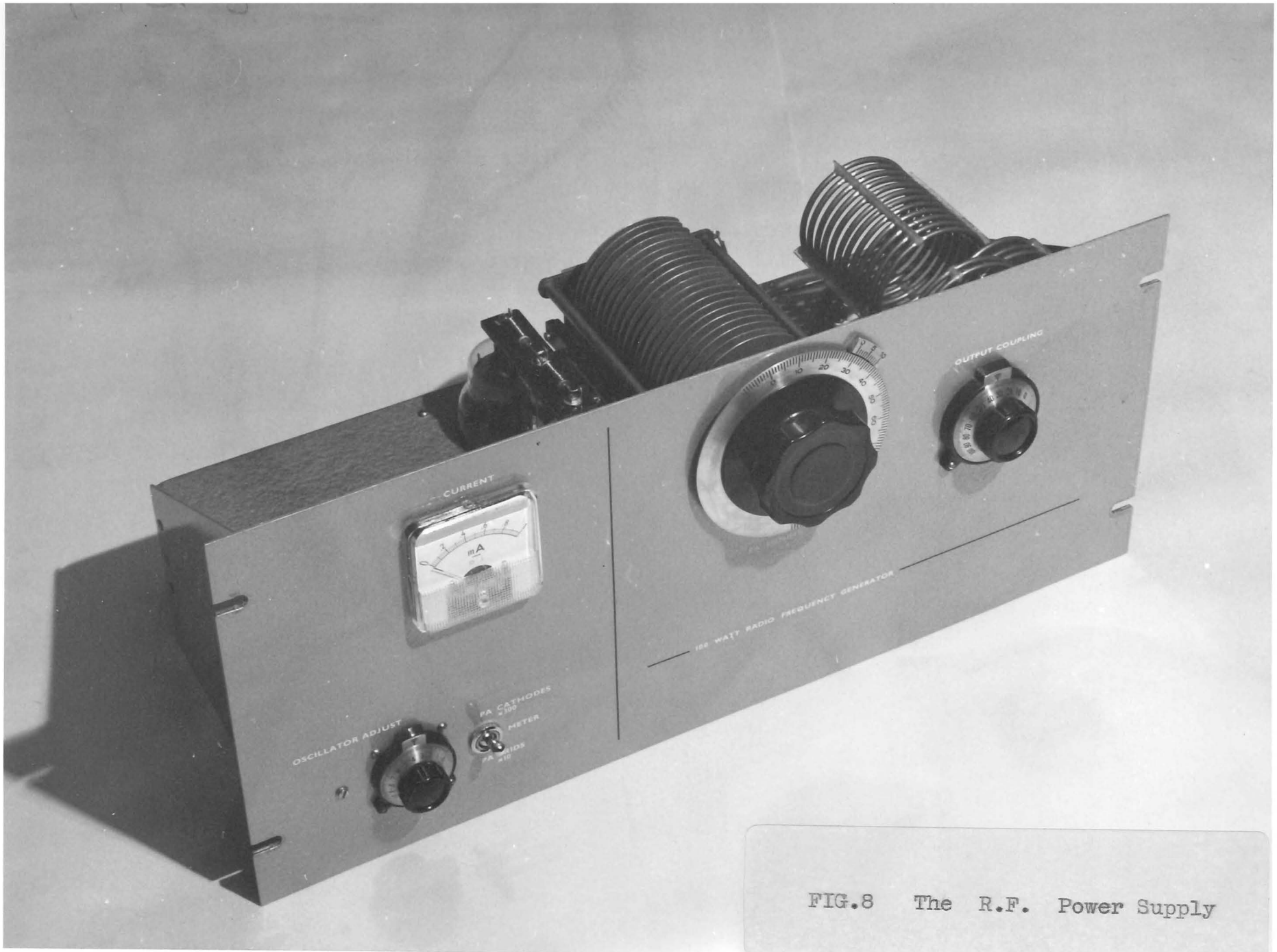

FIG.8 The R.F. Power Supply

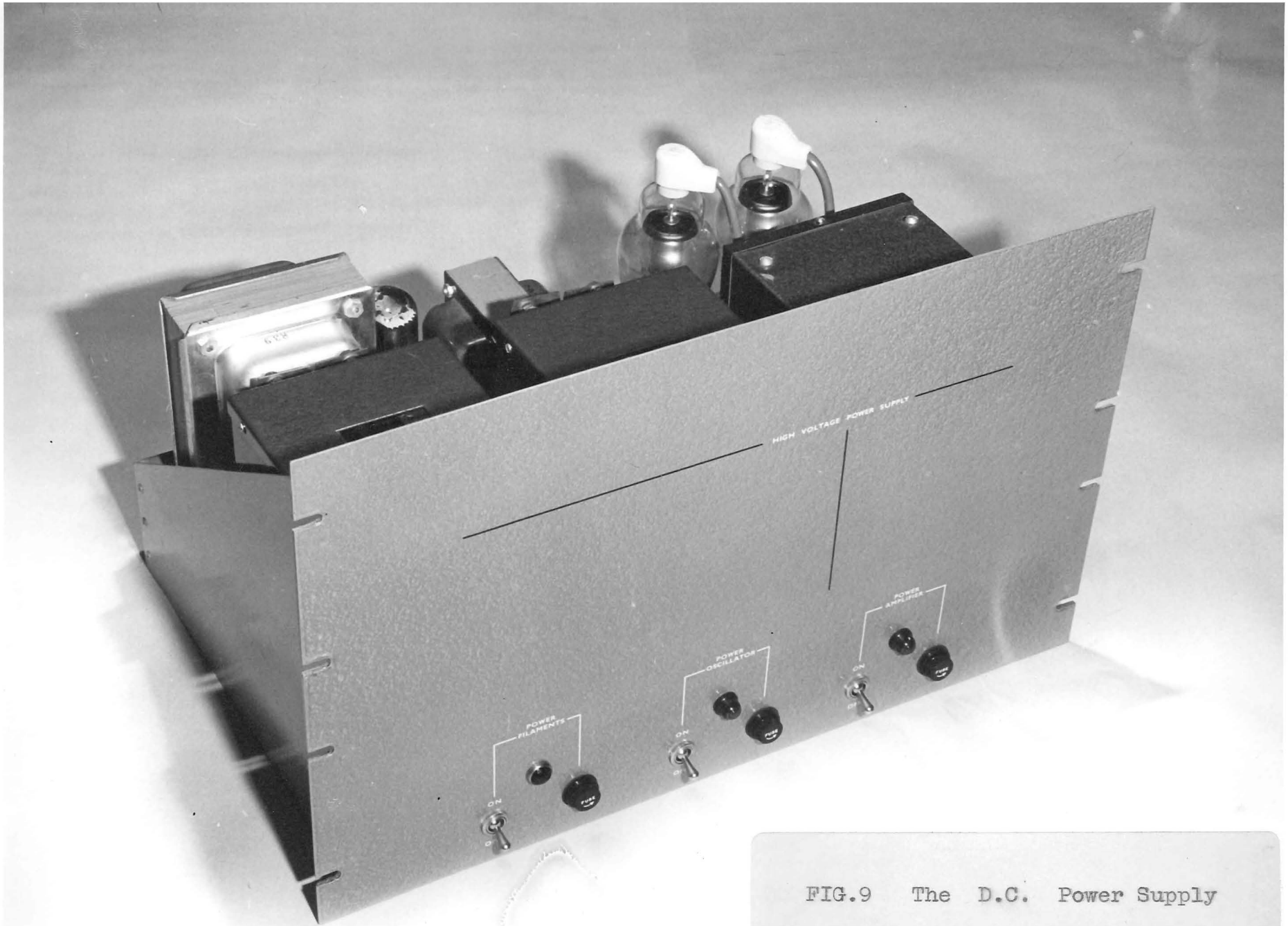

FIG.9 The D.C. Power Supply

Transducer Characteristics

With the R.F. power supply working as planned, a determination of the electrical characteristics of the transducer was necessary to determine the true operating frequency.

Transmission method:

An experiment was performed which gave the transducer frequency response over the frequency range 3 - 7 Mc/sec. The experiment consisted of the following steps.

(1) a constant current of 35 MA (R.M.S) was passed through the transducer (which was mounted in the ultrasonic tank).

(2) at a given frequency, the voltage across the transducer was measured.

(3) step (2) was repeated for different frequencies in the range 3 - 7 Mc/sec.

(4) steps (1), (2) and (3) were carried out first with the ultrasonic tank empty, and then with the tank filled with water.

The results are shown in the graph of Figure 10. (This graph was plotted using the Autoplotter function of the IBM 870 computer system in the University Mobil Computer Laboratory.) The graph shows points of minimum and maximum resistance. However, as Onoe, Tiersten and Meitzler have shown,[16] the transmission method is unsatisfactory as it is

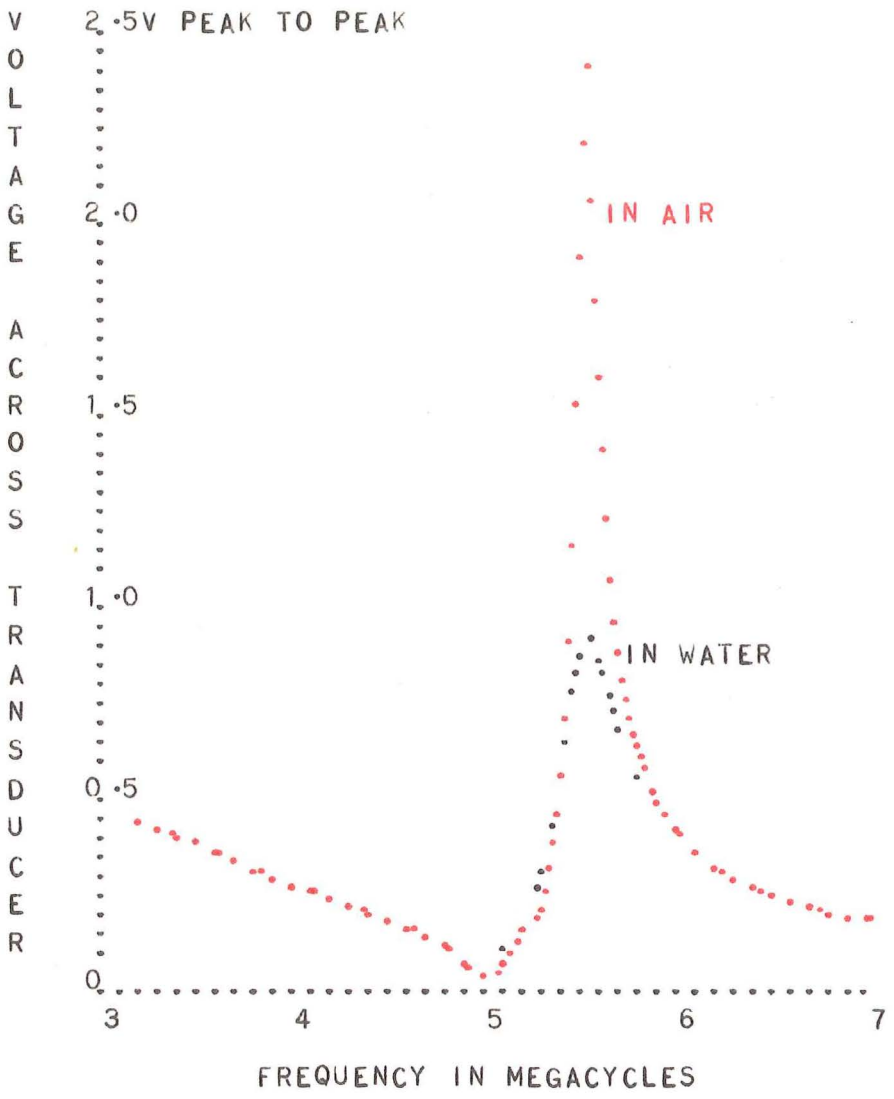

FIG. 10

FREQUENCY RESPONSE OF TRANSDUCER

~~as it is~~ uncertain as to whether these points define the series and parallel resonant frequencies of the transducer. (For a discussion on the resonant frequencies of a transducer see Reference 12, page 109.) However, the results do indicate the lowering in transducer Q due to the loading effect of the water.

Bridge method:

Following the method outlined by Onoe, Tiersten and Meitzler,[16] the equivalent series resistance and reactance of the transducer were read directly from a G.R. Radio Frequency Bridge (Type 916-A) for various frequencies in the range 3 - 7 Mc/sec. The results obtained are shown in the graph of Figure 11. The results indicated that

f_r (series resonance frequency) = 5.00 Mc/sec

f_a (parallel or anti-resonance frequency) = 5.48 Mc/sec

and a position of maximum resistance occurs at a frequency = 5.52 Mc/sec

(This maximum in resistance does not occur at the parallel resonance frequency, and thus the results shown in Figure 10 would give an erroneous value for f_a, the transmission method giving the position of maximum resistance only.)

Note: This experiment was carried out with the transducer in its proposed operating position, i.e., the transducer was mounted in the water-filled ultrasonic tank. This

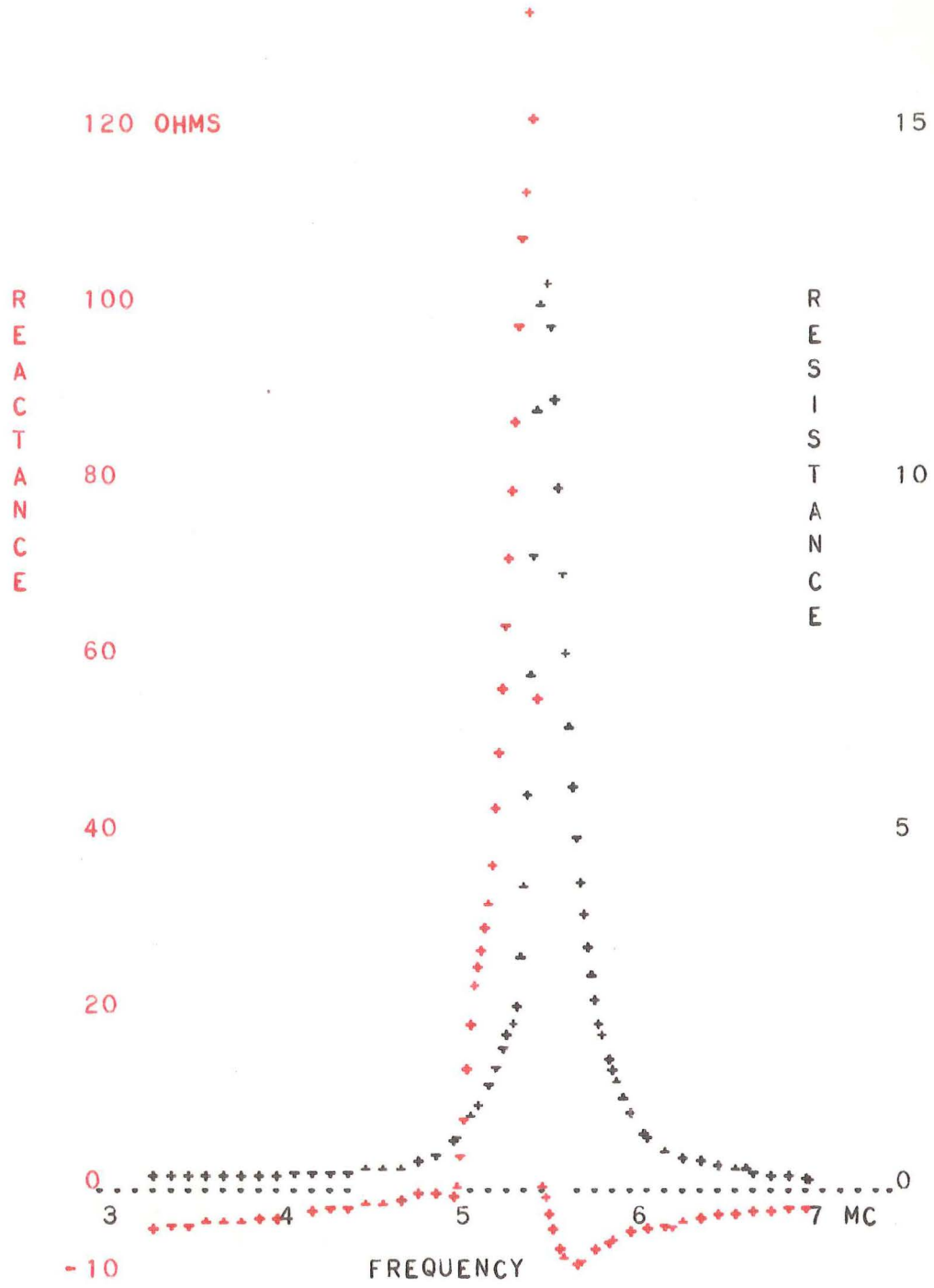

FIG. 11

ELECTRICAL CHARACTERISTICS OF TRANSDUCER

is necessary as the electrical characteristics vary with the transducer loading.

Normally a transducer is operated at its series resonant frequency. However in this case the electrical resistance is very low (less than one ohm) at f_r; whereas at f_a its resistance is 12.5 ohms. Therefore it would be preferable to operate the transducer at f_a rather than f_r as, for the same power input, less current is required at f_a. (Thus the transducer is less likely to be damaged through an excess of current at high power inputs.)

An experiment was performed to determine whether the choice of operating frequency was critical. This experiment consisted of setting up a lens system in conjunction with the ultrasonic tank to observe the Debye-Sears diffraction pattern (as in Fig. 1). For constant power input to the transducer, the number of orders visible was observed at both the frequencies f_r and f_a. The theory being that if more ultrasonic power was produced by the transducer at one frequency compared with the other then more orders would be visible in the diffraction pattern. This follows from the fact that the number of orders visible depends on the intensity of the ultrasonic wave.

The results showed that either frequency was suitable, the number of orders visible being the same in both cases.

Hence, on the basis of the higher transducer resistance at 5.48 Mc/sec, f_a was chosen as the transducer operating frequency.

CHAPTER 3

LIGHT SOURCES AND DETECTORS

For best observation of the Debye-Sears effect the light source should be

(a) collimated

(b) monochromatic--because of the dispersive nature of the ultrasonic grating and

(c) coherent--because the diffraction pattern is produced by the interference of light.

The Laser

A gas laser is such a light source, the light being highly coherent, monochromatic, parallel and continuous. (For a review of laser properties see "Optical Masers" by O. S. Heavens.[17])

Parts for a Helium-Neon gas laser were obtained from Semi-Elements, Inc., these being

(a) a 115 cm-long gas discharge tube with Brewster-angle windows (type number SEOG-t-2). The gas tube contains He-Ne gas in the correct ratio and at the correct pressure.

(b) two 2 inch-diameter concave mirrors of 135 cm radius of curvature. These mirrors are dielectric coated for operation of the laser at 6,328 Å. The concave mirrors produce a slightly divergent laser beam, but the divergence is

negligible over 10 cm (the width of the ultrasonic tank).

Mirror holders and tube mounts were designed and constructed, the result being shown in Figure 12.

Each mirror is held in its brass holder by four nylon-tipped screws. And as the laser is designed to operate in the confocal mode, the holders are separated by a distance equal to the radius of curvature of the mirrors.

Mirror-angle adjustment is by means of two micrometer screws and one fixed screw spaced at 120^{o} intervals around the mirror holder perimeter. The micrometers are ball ended and fit into sockets in the holder, while the fixed screw is cone tipped and fits into a corresponding dent in the holder. Tension between the adjusting screws and the mirror mount is maintained by three steel springs.

The laser tube is supported by three perspex rods with spring clips on the top. These clips serve as tube retainers and as electrodes for the gas discharge. A balanced power input is used, the centre electrode being the "hot" terminal while the two outer electrodes are earthed.

A radio frequency discharge is used to excite the gas for laser action to take place. A 200 watt, 200 kc/sec R.F. supply was available and this was used, although only approximately 60 watts of power should be necessary to obtain laser action. The R.F. supply can be seen in the rear

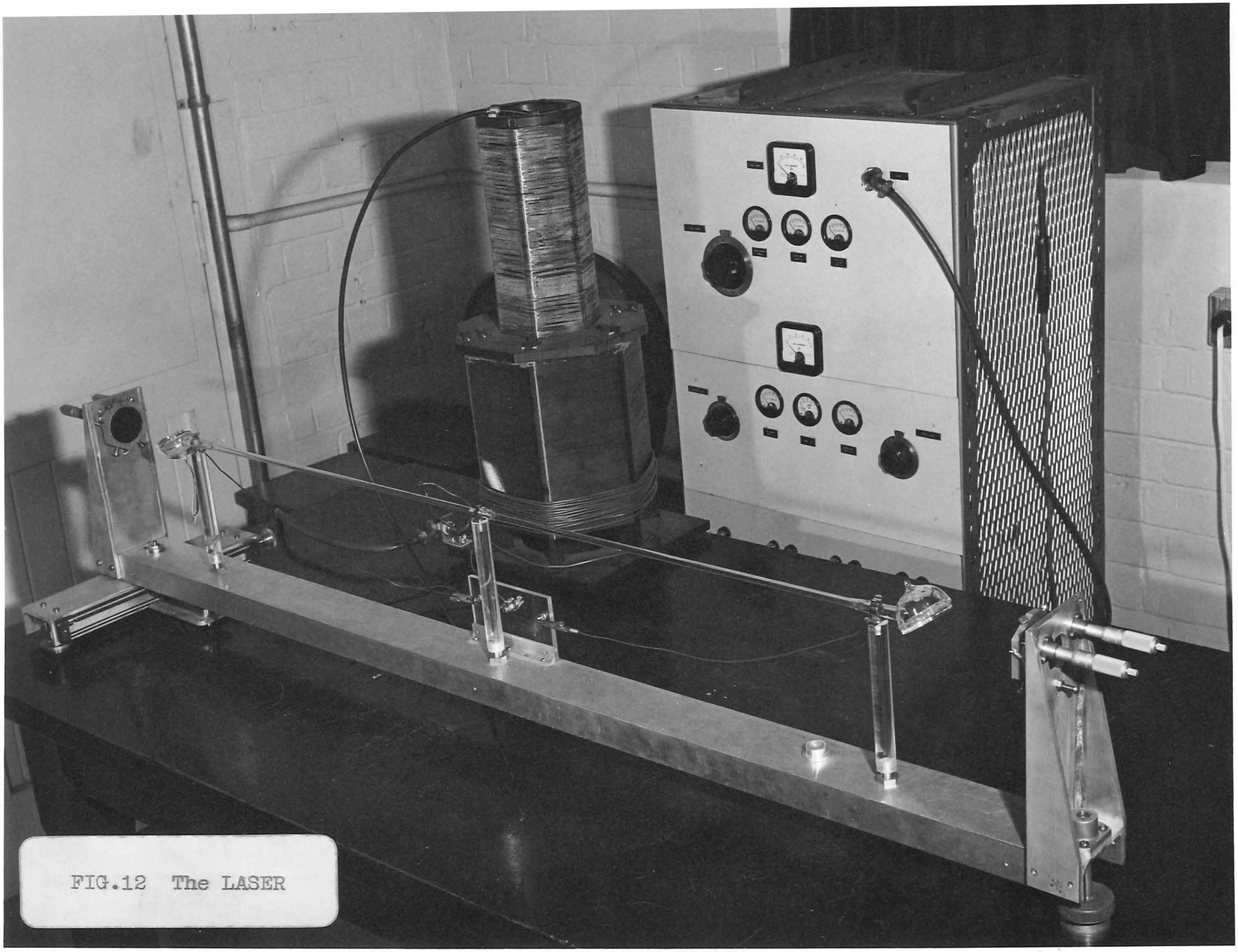

FIG.12 The LASER

of the photograph (Fig. 12). The Tesla coil, visible to the left of the transmitter, is used as a voltage step-up transformer.

A protective perspex cover (not shown in the photograph) slips over the laser and is screwed to the aluminium U channel that forms the base. This base is mounted on a finely adjustable traversing mechanism so that the laser can be pointed with accuracy in any required direction. (This feature is necessary as the angle of incidence need only be varied by several minutes for the Bragg reflection to be apparent in the diffraction of light by ultrasonic waves.[10])

The laser parts arrived late in the year; and, when they did arrive, it was found that a plane mirror had been sent in place of a concave one. A replacement mirror was requested and arrived towards the end of October.

Meanwhile, an unsuccessful attempt was made at obtaining laser action using the plane mirror. The planar-concave mirror system (the hemispherical resonator) is difficult to align compared with the concave-concave mirror system (the confocal resonator). In fact, Bloom[18] recommends that the spherical mirror should first be operated as part of a confocal system when setting up a hemispherical resonator. For this reason further attempts at obtaining laser action were postponed until the concave mirror arrived.

The confocal resonator is the least critical in its alignment requirements of all the gas laser cavities that have been developed.[19] However the separation of the mirrors is critical, the rule for stability being stated by Yariv and Gordon[20] as follows:

> Of the various systems consisting of two curved mirrors, only those systems for which the centre of curvature of one mirror, or that mirror itself, but not both, lies in the region between the other mirror and its centre of curvature are stable and hence suitable for laser cavities.

This means that for stability in the concave-concave mirror system either

$$d < b_1$$

or $$d > b_2$$

if $$b_1 < b_2$$

where d = separation of the mirrors

b_1 = radius of curvature of one mirror

b_2 = radius of curvature of the other mirror.

For the confocal system,

$$b_1 = b_2$$

and hence the system is unstable when

$$d = b_1$$

Thus when the confocal system was set up, the spacing d was adjusted so that it was 1 cm less than the radius of curvature of the mirrors, i.e., d was set at 134 cm.

Alignment of the mirrors was attempted using a technique described by Stong.[21] In this method light is beamed down the laser tube and focussed onto the far mirror. The mirror is then adjusted to return this beam back down the tube. The process is repeated for the other mirror. According to Stong, this method should align the concave mirrors accurately enough for laser action to take place (though a slight movement in the adjusting screws may be required).

Despite careful alignment of the mirrors laser action was not achieved. And such is the case at the time of writing.

The failure to obtain laser action is thought to be due to faults in the mirror mounting method. With the present system, the apparent mirror centre, as viewed down the tube, moves in a circular motion when a micrometer is turned. This is far from the wanted case, which is a pure tilt about the other two suspension points. This defect is probably due to the micrometer balls not fitting true in their sockets. A better mounting system would have all the screws cone tipped and fitting accurately into dimples in the mirror holder. At the same time the springs should be replaced with ones of a higher quality, the present springs having stretched considerably with use.

Further, the radius of curvature of the mirrors should

be checked and the separation distance adjusted to a stable value if necessary. As a final step the reflectivity of the mirrors could be checked for a maximum of 6,328 Å.

An Alternative Light Source

With the laser not "lasing" an alternative light source was required. Three suitable sources were available,

(a) a sodium vapour lamp

(b) a 250 watt mercury vapour lamp

and (c) a mercury vapour point source of the Mazda box type.

A critical evaluation of these sources was carried out.

The sodium lamp was down in intensity compared with the others but has the advantage of being easily monochromated. The mercury point source was unsuitable as its light output visibly fluctuated in intensity over short periods of time. The mercury vapour lamp gave a steady output and filters could be used to monochromate the output without a serious loss of intensity. Of the three, this lamp appeared to be the most suitable.

The Detectors

As a very intense light source (the laser) may be used the detector should be capable of measuring the high light intensity without damage to the detector. The spectral

sensitivity is important only in that the detector should be sensitive to the wavelength of the light being used. The detector should be capable of differentiating between the various orders of the diffraction pattern and faithfully record their intensity.

Three different types of detection were envisaged,

(a) Photomultiplier

(b) Photoresistor

and (c) Photographic.

(a) The Photomultiplier Photometer:

The photomultiplier tube is incorporated in a circuit similar to one described by Bradford.[22] The circuit (Fig. 14) has unique features that make it suitable for this research. A full description of the operation of the circuit, the design considerations, and the characteristics of the photometer can be found in Bradford's paper.

It is sufficient to say that the photometer was the photomultiplier in a feedback circuit which alters the sensitivity of the phototube according to the light level (the phototube is operating in a "constant anode-current" mode). This enables a range of light intensities in excess of 10^9 to be measured on the 0-1 mA current indicating meter. The meter reads inversely; maximum deflection occurring with the photocathode in darkness and minimum deflection at the highest

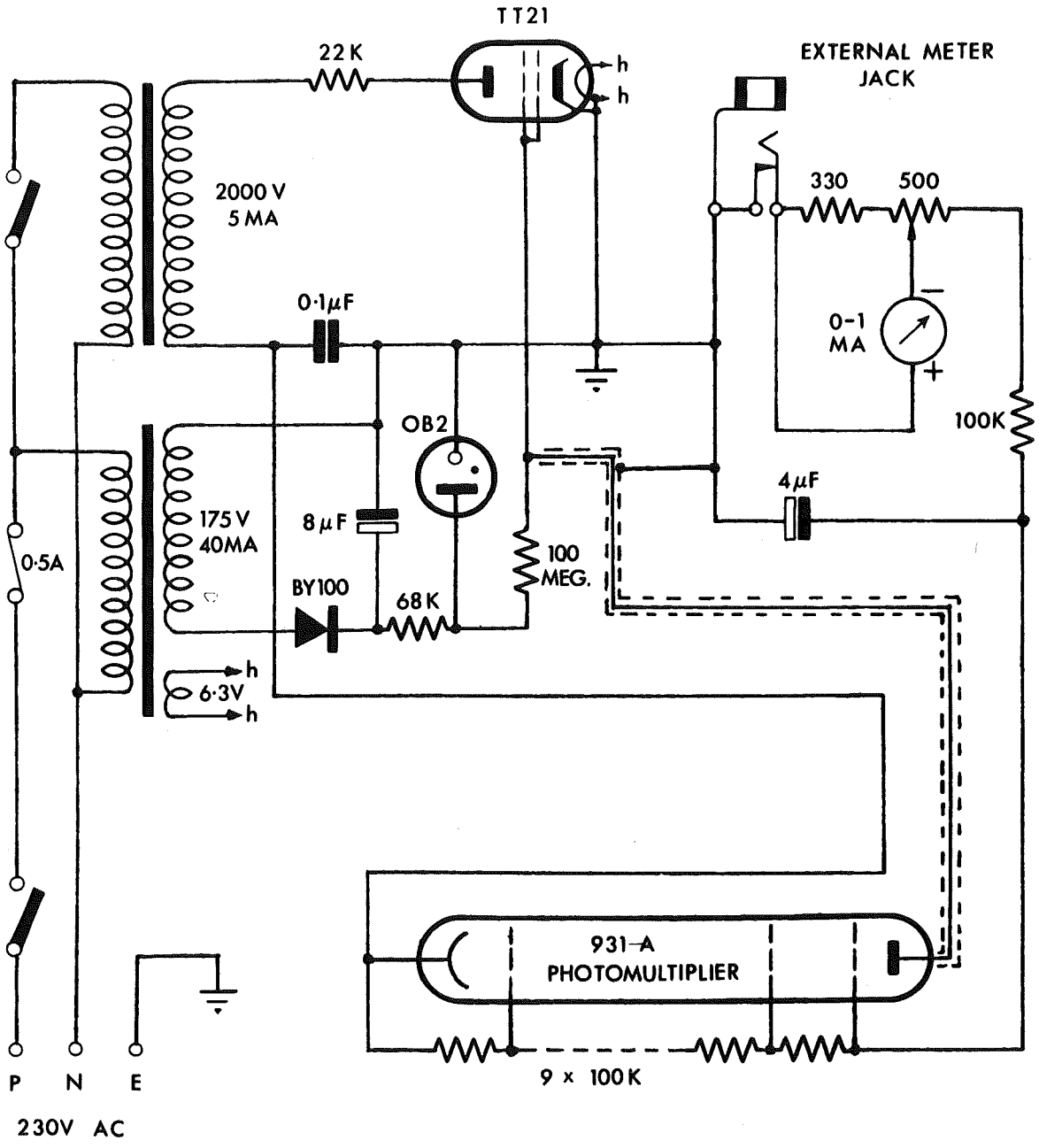

FIG. 14

Circuit of the
Photomultiplier Photometer

light level. The circuit is so designed that it is impossible to drive the meter needle off scale. Nor is it possible to damage the photomultiplier at any light level because of the automatic adjustment of sensitivity.

The use of the phototube in this manner necessitates the loss of its high speed response, though this gives the detector the advantage of being relatively noise free. Because of the slow response to intensity changes, a slow scanning speed will be required when the diffraction pattern is being monitored with this detector.

The instrument is calibrated with the phototube in darkness and involves setting the meter reading to 1 mA by means of the 500 ohm potentiometer.

The phototube was mounted in a light-tight brass housing which also contained the 100,000 ohm voltage-dropping resistors. Wire cables of sufficient length to enable the photomultiplier housing to be moved independently of the main unit provided the electrical connections. A short length of brass tubing forms a circular window in the holder directly opposite the photo-sensitive cathode of the photomultiplier. A Hilger calibrated slit fits snugly over this window.

The spectral response of the photometer depends on the spectral response of the phototube, but, as mentioned before, the light source is monochromatic and the only criterion is

that the phototube be sensitive to the radiation. Unfortunately, the only suitable photomultiplier tubes on hand were the 931-A and an IP 28, both having low sensitivity in the red (4% of maximum sensitivity) as both were designed for a maximum response in the blue-green region of the spectrum. However, a laser beam is very intense and the limited photomultiplier response may be sufficient. The photomultiplier response, as far as the mercury source is concerned, would be more than adequate.

On testing out, the photometer was found to be working to the original specifications, the intensity response being log-linear over the 0.15-0.85 region of the 0-1 mA scale.

(b) The Photoresistor Photometer:

With the response of the photomultiplier photometer to the 6,328 Å laser radiation being an unknown factor, an alternative detector is required.

A cadmium sulphide photoresistor (Philips type number B 8 731 03) is a suitable detector. The spectral response of this detector is peaked in the red at 6800 Å, but it is also adequate in the green. Thus the photoresistor is excellent for laser beam detection work.

The current versus illumination relationship for the resistor is roughly linear for a given applied voltage. Therefore, for a constant voltage across the photoresistor,

the current through the photoresistor (and therefore the resistance) is proportional to the illumination. Hence the method of detection is to simply measure the resistance of the photo-element.

The resistance of the photoresistor ranges from 100 ohms in bright light to 10 million ohms in darkness. Again the response to changes in intensity is slow, the recovery rate being 200,000 ohms/sec, and therefore a slow scanning speed is necessary.

The photoresistor was mounted in a light-tight housing that again incorporated a Hilger adjustable slit. This slit was positioned so that the line of the slit intersected the strips of photosensitive material at right angles.

This method of detection will be used for rough comparisons of intensity, being used for finer work only if absolutely necessary.

(c) The Photographic Method:

The method involves photographing the diffraction pattern with a material of suitable sensitivity, developing the negative, and then using a densitometer to determine the intensity of the various orders.

This method is difficult to carry out in practice as a close control of materials and processing conditions is

necessary if an accurate comparison of intensities is required. Consequently this method is envisaged as being used for checking purposes only.

CHAPTER 4

THE COLLOIDS

The colloids were chosen with regard to the particle shape and the nature of the suspending medium.

As it is more convenient to use one type of liquid only when operating with the ultrasonic tank it was decided that the suspending medium should be water in all cases. With this restriction, six colloids were chosen for manufacture. The colloids, and their particle shapes, are listed below.

Colloids chosen for preparation	Particle shape
Red gold	Spherical
Sulphur	"
Aged hydrous ferric oxide	Plate-like
Blue gold	"
Aged vanadium pentoxide	Needle-like
Aniline blue dye	"

Preparation of the Colloids

The basic recipes for all sols except aniline blue came from "Experiments in Colloid Chemistry" by Hauser and Lynn.[23] These basic recipes were tried, and if the resulting sol was not satisfactory the formula was altered. In most cases these alterations amounted to an increase in the chemical quantities so that a more concentrated sol was obtained.

The colloid samples were prepared using the following recipes.

Red Gold Sol:

Heat a mixture of 1 ml of a 1% gold chloride solution and 200 ml of distilled water to 60°C. Then add 10 ml of a freshly prepared 0.1% tannic acid solution with vigorous stirring.

Sulphur Sol:

Add 2 gm of sulphur flowers to 50 ml of 95% ethyl alcohol. Shake throughly and repeatedly for 15 minutes and filter. Slowly add 10 ml of the filtrate to 200 ml of distilled water, stirring constantly.

This sol is unstable, the sulphur gradually settling out of solution over a period of several weeks.

Hydrous Ferric Oxide Sol:

Add 1 ml of a 60% ferric chloride solution to 250 ml of boiling water. Continue boiling, replacing water lost by evaporation, until a clear red sol is obtained (usually within half an hour).

Blue Gold Sol:

Add 1 ml of a 1% gold chloride solution to 200 ml of distilled water. Mix thoroughly. Add 10 ml of a very dilute hydrazine sulphate solution (three small crystals of hydrazine sulphate in 50 ml of distilled water) and heat for a few minutes.

This sol is unstable and the gold particles will settle out of solution in time.

Vanadium Pentoxide Sol:

Mix, by means of a mortar and pestle, 4 gm of ammonium vanadate and 25 ml of dilute (3N) hydrochloric acid. Place the mixture on a filter and wash until the filtrate begins to come through the filter a distinct red colour. Wash the precipitate off the filter into a beaker and make up the volume to 200 ml with water. The precipitate will gradually disperse over a period of 12 hours.

Aniline Blue Sol:

Add 0.05 gm of aniline blue (water soluble) to 200 ml of water, with stirring.

(This is the only sol of the six which is not lyophobic in nature. Aniline blue is a dye and therefore is classified as a colloidal electrolyte.)

A simple experiment was performed on each sol to determine whether or not the desired particle shape had been achieved. The experiment was to observe the behaviour of the sol in polarised light, the theory being that non-spherical particles show "streaming double refraction" when stirred.

The apparatus consisted of a strong white light source which shone in the direction of a pair of crossed polaroids. The sol was inserted between the polariser and the analyser and observed through the analyser. If the particles of the

sol were non-spherical, then stirring the sol would produce a bright field in the analyser in place of the normal dark field.

The result of this test, together with a summary of the physical appearance of the sols, is given in Table 1.

TABLE 1

Result of the "Stream Double Refraction" Test

Sol	Colour of the sol by transmitted light	Result of the double refraction test
red gold	purplish-red	negative (as expected)
sulphur	opaque white	not tested as too opaque
ferric oxide	reddish-brown	negative
blue gold	light blue	positive (but doubtful)
vanadium pentoxide	bright red	positive
aniline blue	deep blue	negative

The ferric oxide sol was not expected to give a positive test as considerable ageing of the sol is required before it becomes doubly refracting. (Some texts recommend a standing period of as much as one year.) A forced ageing was tried by boiling the sol for some five hours, but with no success. This boiling had the effect of deepening the colour of the sol; and, in reflected light, the previously clear reddish-brown solution had become brown and opaque. This would indicate that the particles had grown in size. However, the double refraction

test still gave a negative result and this would indicate that the growth was not in the required plate-like form.

Blue gold sol, though giving a doubtful result in the double refraction test, could be assumed to have plate-like particles as it has been shown that the blue colour of the sol is dependent on this type of particle.[24]

The vanadium pentoxide sol required a premature ageing (by boiling for one hour) before it showed streaming double refraction. This was the only colloid to give a definite positive result on testing.

CHAPTER 5

EXPERIMENTS AND RESULTS

The object of this research is to investigate the behaviour of colloids in a sound field by observing their action on the diffraction of light by ultrasonic waves. The experiment requires the use of a suitable light source, and an ultrasonic tank, to obtain the Debye-Sears diffraction pattern. Colloids will then be added to the water in the tank and any change in the diffraction pattern noted.

The Experimental Arrangement

The apparatus required for the experiment was set up as shown in the block diagram of Figure 15. Most of the equipment used has been described previously.

The Radio Frequency supply delivers power to the transducer in the ultrasonic tank. The oscilloscope (Telequipment Serviscope type D31) is used to monitor the voltage across the transducer. This voltage gives an indication of the intensity of the sound waves and enables measurements to be repeated at the same sound level.

The light source was to be the 250 watt mercury vapour lamp used in conjunction with a set of lenses and a slit to produce the required parallel light (as in Fig. 1, with lenses L_1, L_2 having a focal length of 10 cm).

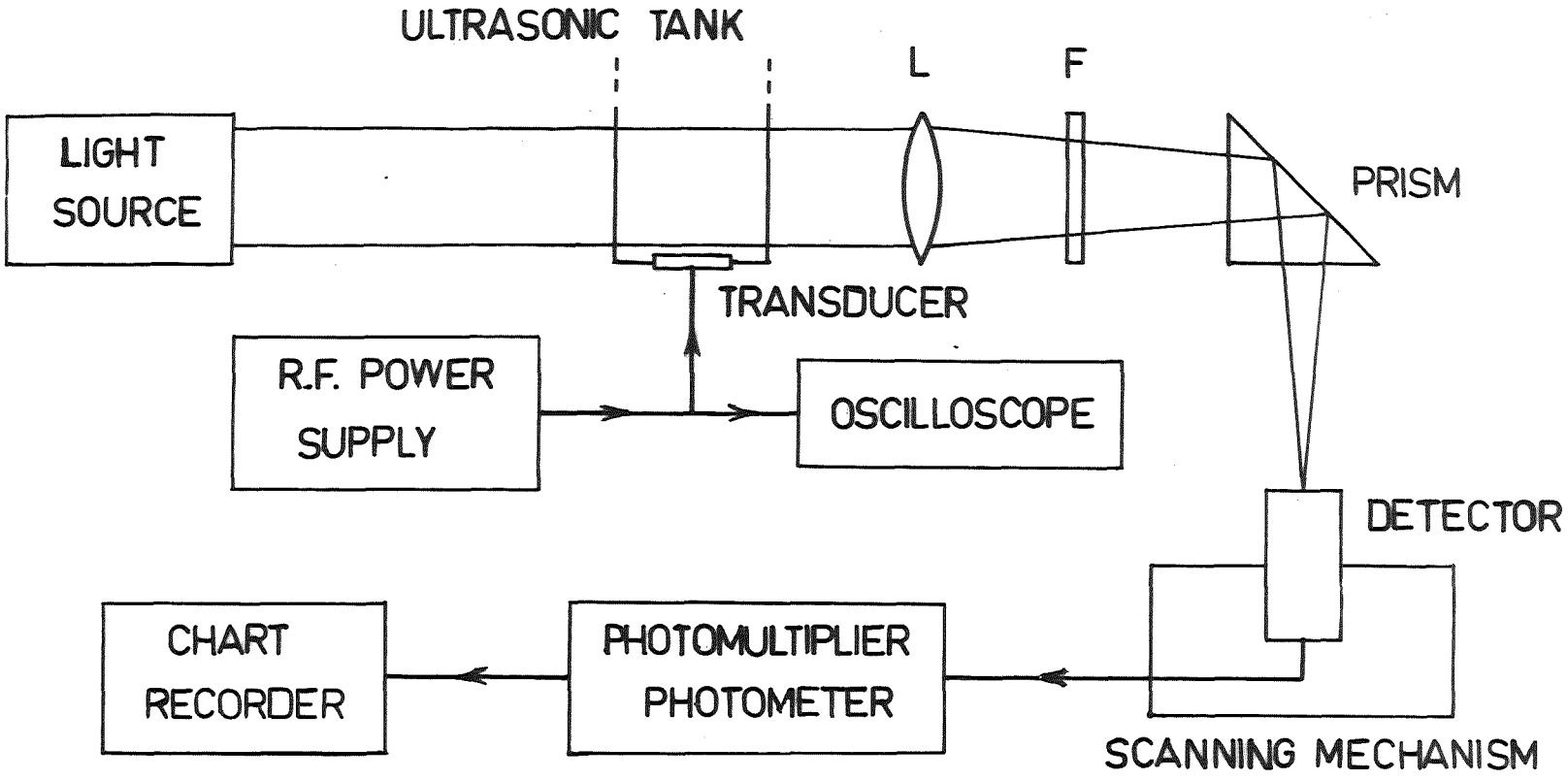

FIG.15

BLOCK DIAGRAM OF THE EXPERIMENTAL ARRANGEMENT

However, at a late date, a commercially built gas laser arrived and was made available for this research. This laser (a NELAS Laser, model G1) was already constructed, complete with its own R.F. power supply, although the concave mirrors required alignment.

Mirror Alignment:

The mirrors were aligned using the technique of beaming the light from a 6V lamp filament down the laser tube. In this case, the light was shone through one mirror and down the tube to the other mirror. This mirror was adjusted to reflect the light back down the tube. The mirror nearest the light source was then adjusted to return the reflected light back down the tube. (Observing the light source through the far mirror would thus produce two images of the filament; one image being inverted and down in intensity compared with the other.)

The alignment achieved in this manner was sufficiently accurate for laser action to be obtained when the 30 Mc/sec R.F. power was applied to the gas tube.

Laser Beam Characteristics:

An intense red beam of light at 6,328 Å is produced by the laser, together with a dispersed blue background illumination. The blue light was produced by non-coherent light from the discharge passing through the concave mirrors.

Chance-Pilkington glass filter, type OR1.

The prism is used to deflect the light through 90^{o} towards the detector. (This feature is for operating convenience only.)

The photomultiplier section of the photometer is mounted on a motor-driven traversing mechanism that enables the detector to scan the diffraction pattern.

The output of the detector is fed to a chart recorder (Heathkit type EUW-20A).

Figures 16 and 17 are photographs of the experimental arrangement.

In Figure 16 are shown, from left to right, the chart recorder (though the one shown, a Varian recorder, was not the one used in the experiment); the photomultiplier photometer; the photoresistor photometer with its resistance measuring meter in back of it; the photomultiplier housing with the oscilloscope behind it; the ultrasonic tank; and the optical system. Below the tank can be seen the transducer power supply. (Neither the laser light source, nor the photo-multiplier traversing mechanism, is shown in this photograph.)

With the experimental arrangements complete, several preliminary runs were made to determine the behaviour of the apparatus.

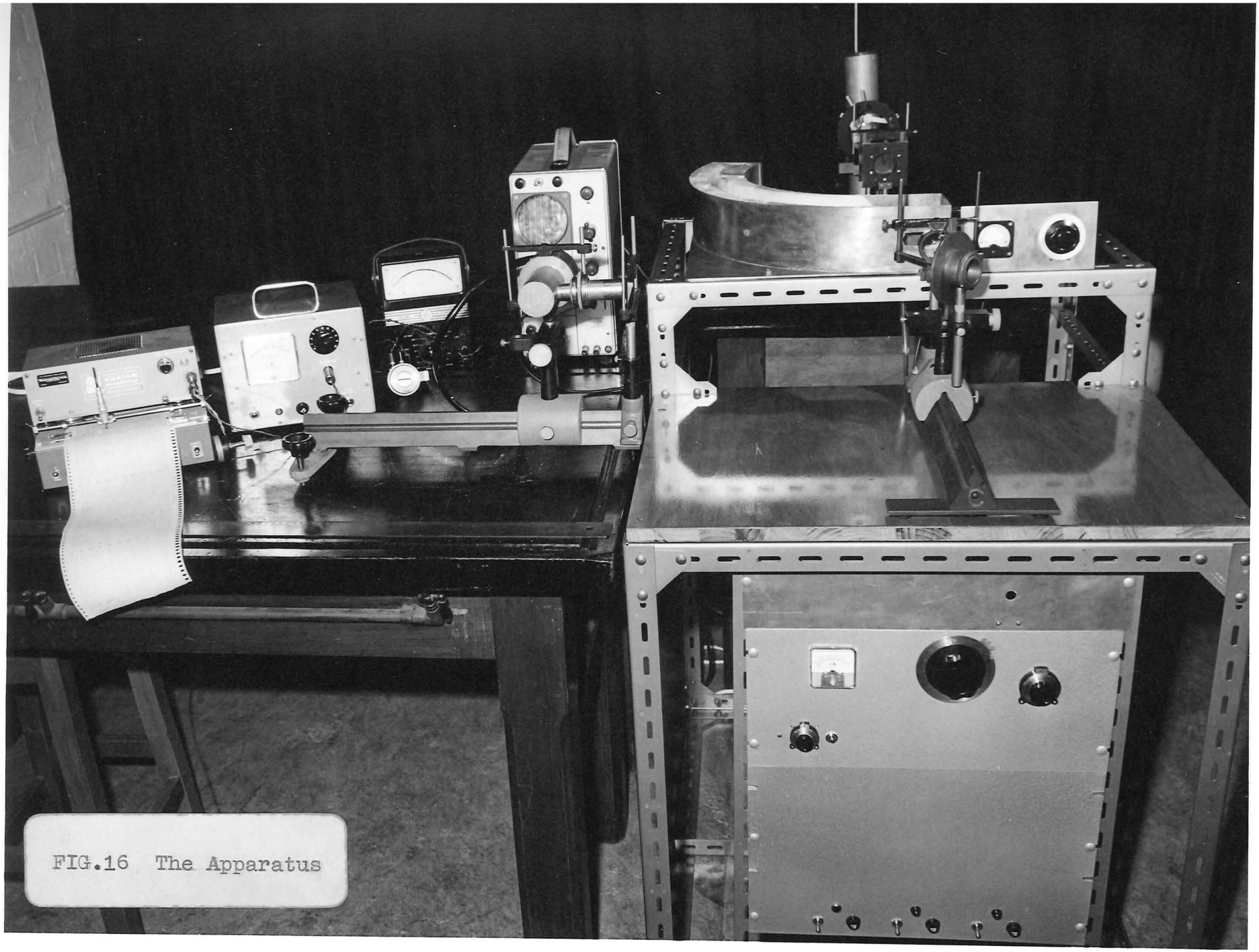

FIG.16 The Apparatus

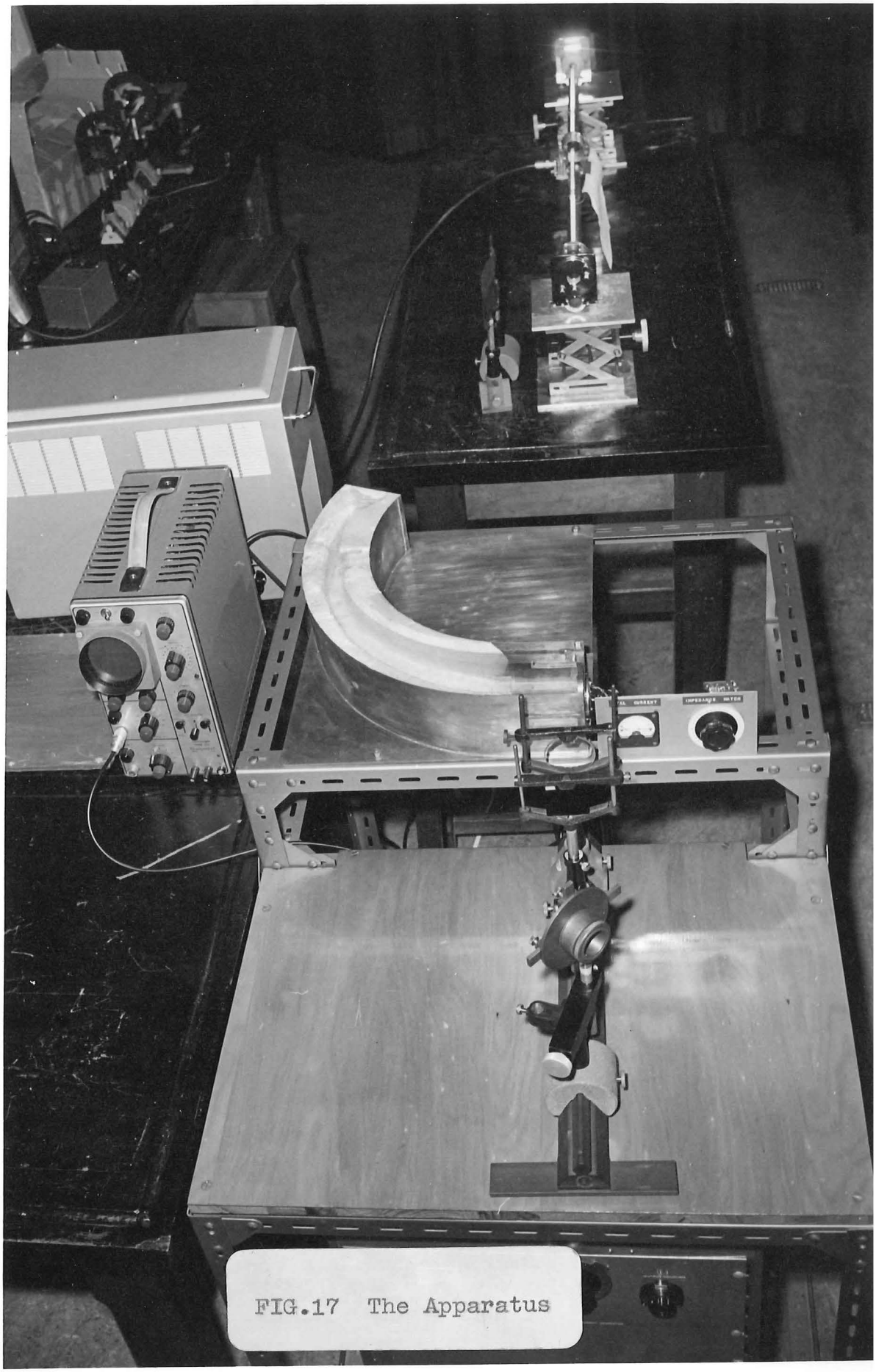

FIG.17 The Apparatus

The ultrasonic tank appeared to be producing the required progressive sound waves. When the tank was constructed a test was carried out before the lining was inserted. The optical arrangement for observing the Debye-Sears phenomenon was set up, and it was found that the diffraction pattern became indistinct at high sound intensities. However, with the lining in place, the tank now gave distinct diffraction orders at the highest sound intensities (corresponding to a transducer input power of 70 watts).

Both the photometers operated as expected, with the photomultiplier photometer proving to possess an adequate sensitivity to the laser light. (A blue filter was used to monochromate the mercury lamp when this source was being used.)

The slit on the detector was opened 10 divisions (equivalent to a slit width of 0.2 mm) and this opening was much narrower than the light peaks in the diffraction pattern which were approximately 2 mm thick. The light peaks were separated by darker regions of similar size.

Photographs of the diffraction patterns that were obtained using the laser light source are shown in Figure 18. The very bright orders in these photographs have overexposed the film, producing a slightly larger image than the true size.

The scanning system worked well, a scanning speed of 1 cm/min being used. At this speed the intensity peaks of

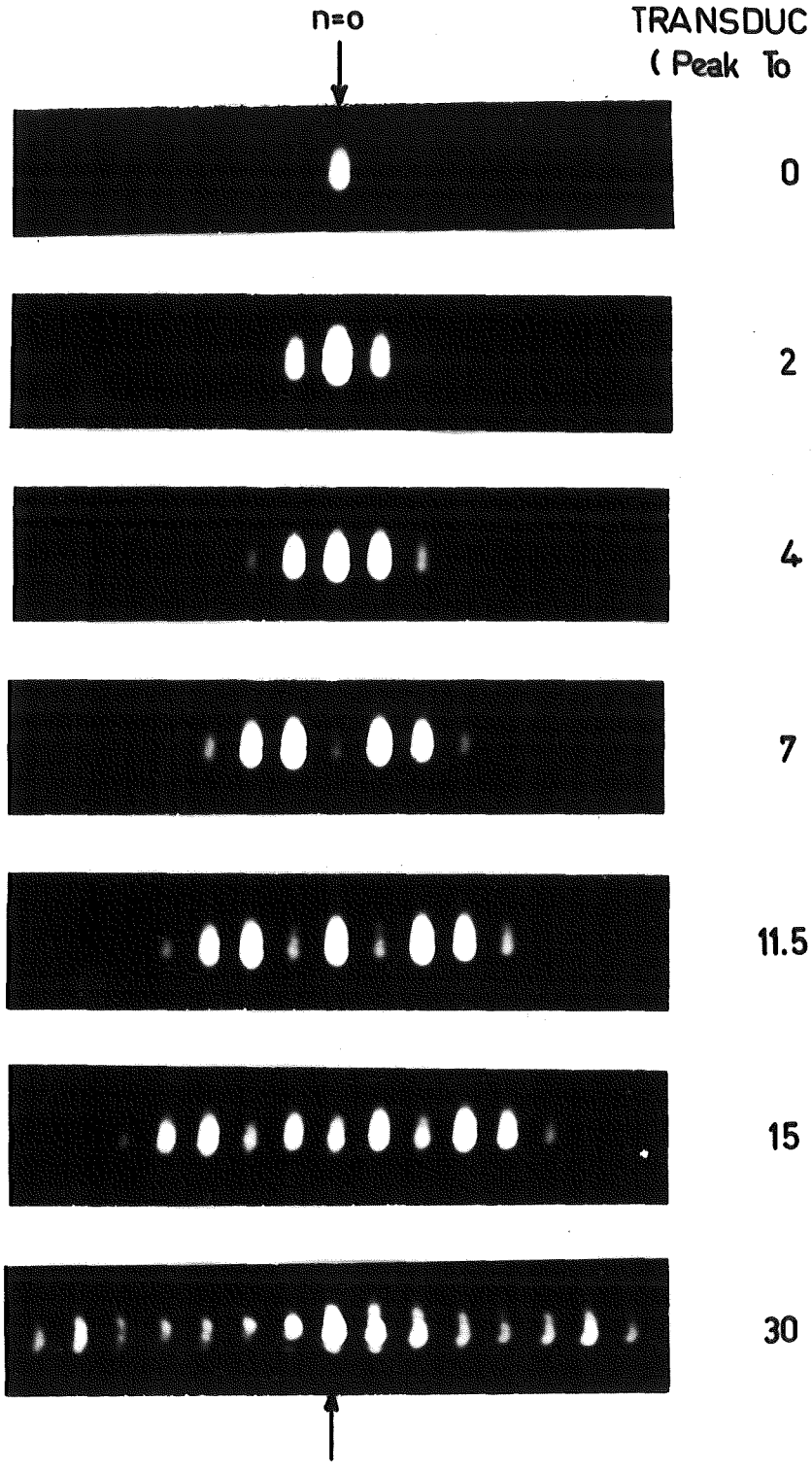

FIG.18

Typical diffraction patterns obtained with the laser light source

the diffraction pattern could be recorded; whereas a faster speed would not allow the photometer-chart recorder system sufficient time to respond to the full variation in intensity.

The diffraction patterns produced by both light sources were scanned, and the advantage of using a Laser light source was immediately apparent. With the mercury source, the spaces between orders in the diffraction pattern were not dark due to imperfect interference of the non-coherent light. A high background level, as much as half of the intensity of the light in the orders, was recorded. With the coherent laser light, however, the dark regions in the pattern recorded at a much lower level.

The Experimental Method

The equipment was calibrated (after a warm-up period of one hour) in the following manner.

(a) the oscilloscope calibration was checked using a 1 volt peak to peak test signal.

(b) the chart recorder was zeroed with its input terminals short-circuited.

(c) the detector slit was closed, and with the photo-multiplier in darkness, the photometer was calibrated to read 1 mA by means of the calibration control.

(d) calibration (c) was transferred to the chart recorder by means of a 100 ohm potentiometer wired into the

external meter socket of the photometer. The input to the chart recorder is taken from the voltage developed across this resistor. The resistor was adjusted so that the chart recorder read full scale (equivalent to 100 mV across the potentiometer).

The slit was then opened to a width of 0.2 mm, to give a photometer reading of approximately 0.95. (This is the background reading for the darkened room.)

The laser light was then shone through the tank, close to the transducer and at centre height. (A distance of 5 mm separated the transducer from the light beam.) The beam was directed close to the transducer to reduce the effect of finite amplitude distortion which would produce an asymmetry in the diffraction pattern.[8]

Using a method outlined by Mayer,[26] the light beam was aligned perpendicular to the direction of propagation of the ultrasonic waves. In this method, the intensity of the $n = \pm 1$ orders of the diffraction pattern are measured and compared at various sound levels and the angle of incidence adjusted until their intensities are equal. At this point the incident light is parallel to the ultrasonic wave front.

The diffraction pattern was recorded for transducer voltages of 0, 4, 8 and 12 V peak to peak. At these low voltages finite amplitude distortion is reduced to a minimum, but the effect of varying the sound intensity can still

be seen. Scans of the diffraction pattern can be made in either direction as the motor is reversible. Hence the records were made with alternate directions of scan (i.e., 0 V record in one direction, the 4 V record in the other, etc.). The 0 V readings were taken as a check on the light beam intensity so that direct correlations between records could be made if necessary.

Experimental runs were taken with (a) water and (b) colloids in the tank. The colloids were slowly, but continuously, fed into the water-filled tank by means of a burette. The burette mouth was placed directly over the transducer so that the progressive sound waves fed the colloids into the light beam. The tank water was replaced before each new experimental run was carried out.

Some typical recordings are shown in Figures 19, 20 and 21.

Recordings were made for all colloids except sulphur and vanadium pentoxide. The sulphur sol was not suitable as the sulphur had precipitated out of solution. The vanadium pentoxide sol gelatinized on contact with the water in the tank and thus was of no use. However, the thin filaments of vanadium pentoxide gel did show the progressive nature of the sound waves as the filaments were suspended in the water at transducer height and gradually moved down the tank in a continuous streamer under the action of the ultrasonic wave.

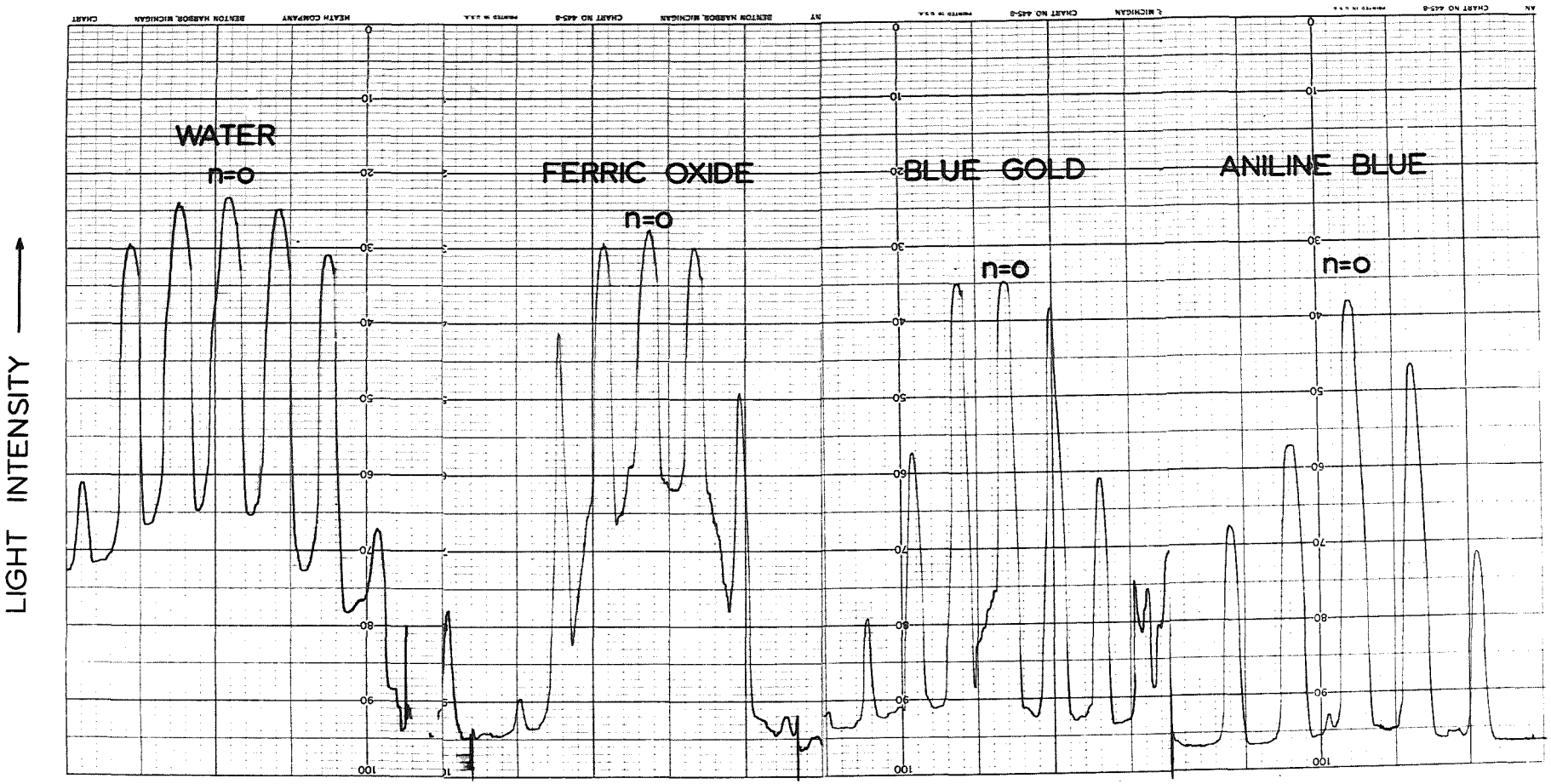

FIG. 19

SOME EXPERIMENTAL RESULTS FOR A TRANSDUCER VOLTAGE OF 4V.

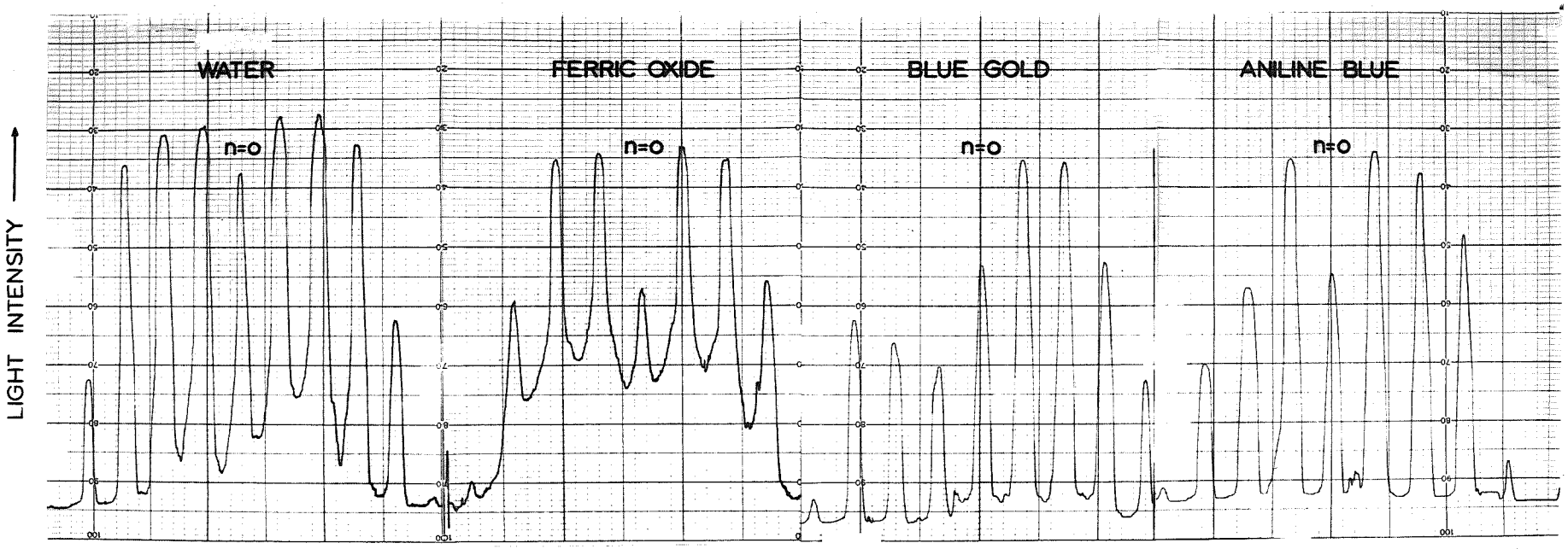

FIG. 20

SOME EXPERIMENTAL RESULTS FOR A TRANSDUCER VOLTAGE OF 8V.

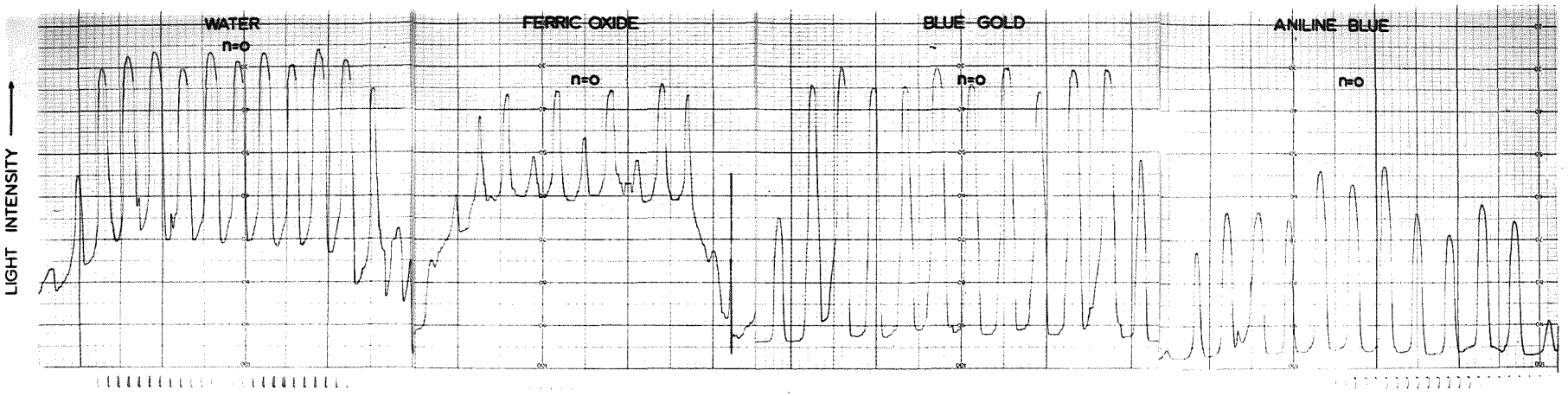

FIG. 21

SOME EXPERIMENTAL RESULTS FOR A TRANSDUCER VOLTAGE OF 12V.

Source of Error

There did not appear to be any error introduced into the recordings by a drifting of the calibration marks. The photometer and chart recorder calibration was checked throughout the experiment and did not show any variation.

The main cause of any error in the results would be the sensitivity of the photometer recording to movements of the supporting table. The floor under this table was not very stable and people moving over this region cause the floor to sag. Consequently the table moves and upsets the alignment of the photomultiplier with respect to the diffraction pattern. This source of error was largely removed by excluding other persons from the area and making sure that the operator remained stationary while a recording was in process.

The chart recorder was capacity sensitive and gave blips on the chart whenever the motor or control knobs were touched. These effects were of no importance provided nothing was touched while a diffraction pattern was being recorded.

However, the motor produced some noise in the chart recordings in one direction of scan only. The electrical noise was picked up by the recorder itself and was due to the motor brushes sparking badly for one direction of rotation only. (This is due to physical limitations in the motor, which was not originally designed to be reversible.) Most of the noise was damped out of the recording by means of a damping

control on the chart recorder.

Another slight error in the recordings could have been introduced by speed fluctuations in the motorised drive. Particularly so in cases where the motor speeds up just as the photometer is about to record an intensity peak. However, the intensity peaks, as recorded, were sufficiently broad at the top to indicate that the intensity maximum had been recorded. As the experiment is one of intensity comparison only, and not of the spacing of orders, this speed variation could be neglected.

CHAPTER 6

DISCUSSION

The diffraction pattern recordings obtained for the various colloids, and sound intensities, are compared with the readings obtained with water in the ultrasonic tank. Comparing each set of results for each colloid in turn, we find that for

(a) Red gold (particle shape - spherical)

The results correlate exactly with those for water. This is to be expected, as the gold particles are approximately spherical in shape and thus no particle alignment would take place.

(b) Hydrous ferric oxide (particle shape - plate-like)

For a transducer voltage of 4 V (peak to peak), the $n = \pm 2$ orders are down in intensity compared with water (see Fig. 19).

At 8 V, the orders $n = 0, \pm 3$ are down in intensity (see Fig. 20).

At 12 V, orders $n = 0, \pm 2, \pm 5$ are down in intensity (see Fig. 21).

In all cases the background light level has gone up, and this is probably due to forward scattering of the light by the ferric oxide particles.

(c) Blue gold (particle shape - plate-like)

For a transducer voltage of 4 V, the $n = \pm 2$ orders are down in intensity compared with water.

At 8 V, orders $n = 0, \pm 3$ are down in intensity, although the first two left-hand orders (Fig. 20) do not show the expected symmetry. (Their lack of intensity may be due to a temporary drop in the intensity of the light source.)

At 12 V, the record is similar to that for water, possibly because the gold particles had moved away from the transducer region. (The flow of blue gold sol into the tank had ceased before this record could be taken.)

In these records, the background level is very low.

(d) Aniline blue (particle shape - needles)

At a transducer voltage of 4 V, no particular order effect is visible. However, the side orders are down in intensity, and it appears that as the n number of the order increases, the drop in intensity (compared with water) increases. This is probably due to increased absorption of the light in these orders by the blue-coloured sol.

At 8 V, orders $n = 0, \pm 4$ are down in intensity. The effect visible in the 4 V record is again apparent, the intensity of the orders steadily dropping off as n increases.

At 12 V, orders $n = 0, \pm 3$ are obviously down in intensity. The effect visible in the 4 V record is again apparent.

In these records, the intensity peaks are reduced in intensity (compared with water) because of heavy absorption

of the light by the blue sol. Again the background level is low, and, as this was also the case with the blue gold sol, it appears that this is due to the blue colour of the sol.

The results obtained for the ferric oxide sol and the blue gold sol, which have a similar particle shape, show some similarity, particularly in the case of the 4 V and 8 V records. Unfortunately, the effect of the aniline-blue needles on the diffraction pattern could not be confirmed as the vanadium pentoxide sol was unusable (as mentioned previously).

In conclusion then, this investigation has shown that plate- and needle-shaped colloids are affected by ultrasonic waves. This is evidenced by a lowering in intensity of particular orders of the Debye-Sears diffraction pattern. At present, there is not sufficient evidence to formulate any theory as to what is happening to these colloids. (In fact, the lack of information, and confirmation, makes the above conclusion a doubtful one.)

Further information could possibly be gained from future experiments if the following lines of approach were investigated.

(a) A repetition of the above experiments, but this time using colloid samples of well defined particle shape under carefully controlled experimental conditions.

(b) Vary the angle of incidence of the light to see if a Bragg reflection is present at a 5 Mc/sec sound frequency when the colloids are added. (This method was not attempted in the present investigation as the angle of incidence could not be varied with any accuracy.)

(c) Increase the sound frequency to 15 Mc/sec so that the Bragg reflection is evident, and then observe if the intensity of the Bragg order is raised by addition of plate-type colloids (as would be expected).

(d) Use a polarised light source, and an analyser, to investigate possible polarising effects produced by the double refraction phenomenon exhibited by aligned colloids. (The laser is a polarised light source, because of its Brewster angle windows, but may not be suitable if the plane of polarisation needs to be rotated.)

REFERENCES

1. H. Dieselhorst and H. Freundlich; Physik Z. 17, 117 (1916).
2. O. Wiener; Kolloidchem. Beihefte 23, 189 (1927).
3. J.W. McBain; "Colloid Science" (D.C. Heath and Co. 1950), p. 97.
4. E.G. Richardson; "Ultrasonic Physics" (Elsevier Publishing Co. 1952), p. 261.
5. S. Oka; Kolloid Z. 87, 37 (1939).
   Z. Physik 116, 632 (1940).
6. P. Debye and F.W. Sears; Proc. Nat. Acad. Sci. 18, 410 (1932).
7. C.V. Raman and N.S.N. Nath; Proc. Indian Acad. Sci. 2A, 413 (1935).
8. E.A. Hiedemann and K.L. Zankel; Acustica 11, 213 (1961).
9. H. Cummins, N. Knable, L. Grampel and Y. Yeh; Applied Phys. Letters 2, 62 (1963).
10. W.G. Mayer; J. Acoust. Soc. Am. 36, 779 (1964).
11. M.A. Breazeale and E.A. Hiedemann; J. Acoust. Soc. Am. 33, 700 (1961).
12. T.F. Hueter and R.H. Bolt; "Sonics" (John Wiley & Sons, Inc. 1962), p. 203.
13. A.E. Crawford; Brit. J. Appl. Phys. 12, 529 (1961).
14. B.E. Noltingk; J. Brit. Inst. Radio Eng. 11, 11 (1951).

15. R. Lipnick, A. Reich and G.A. Schoen; Proc. IEEE 52, 853 (1964).

16. M. Onoe, H.F. Tiersten and A. H. Meitzler; J. Acoust. Soc. Am. 35, 36 (1963).

17. O.S. Heavens; "Optical Masers" (Methuen & Co. Ltd. 1964).

18. A.L. Bloom; Spectra Physics Laser Technical Bulletin, No. 2.

19. D.C. Sinclair; Applied Optics 3, 1067 (1964).

20. A. Yariv and J.P. Gordon; Proc. IEEE 51, 4 (1963).

21. C.L. Stong; Scientific American 211, 227 (Sept. 1964).

22. W.R. Bradford; "Symposium on Astronomical Optics and Related Subjects", Z. Kopal ed. (North-Holland Pub. Co. 1956), p. 244.

23. E.A. Hauser, J.E. Lynn; "Experiments in Colloid Chemistry" (McGraw-Hill Book Co., 1940).

24. H.B. Weiser; "Inorganic Colloid Chemistry" Vol. 1 (John Wiley & Sons, 1933).

25. J.P. Goldsborough; Applied Optics 3, 267 (1964).

26. W.G. Mayer; J. Acoust. Soc. Am. 35, 1288 (1963).

BIBLIOGRAPHY

A list of general references on topics discussed in this thesis:

Clays:

R.E. Grim, "Clay Mineralogy" (McGraw-Hill, 1953).

H. van Olphen, "An Introduction to Clay Colloid Chemistry" (Interscience, 1963).

Colloids:

J.W. McBain, "Colloid Science" (D.C. Heath & Co., 1950).

Streaming Double Refraction:

H.R. Kruyt; "Colloid Science" (Elsevier Publishing Co., 1952), Chapter 3.

Ultrasonics:

E.G. Richardson, "Ultrasonic Physics" (Elsevier Publishing Co., 1952).

T.F. Hueter and R.H. Bolt, "Sonics" (John Wiley and Sons, 1962).

K.F. Herzfeld and T.A. Litovitz, "Absorption and Dispersion of Ultrasonic Waves" (Academic Press, 1959).

Transducers:

W.P. Mason, "Piezoelectric Crystals and their Application to Ultrasonics" (D. Van Nostrand, 1959).

"Physical Techniques in Biological Research" Vol. IV, W.L. Nastuk, Ed. (Academic Press, 1962); Chapter 6 (W.J. Fry and F. Dunn, "Ultrasound: Analysis and Experimental Methods in Biological Research").

Lasers:

O.S. Heavens, "Optical Masers" (Methuen Monograph, 1964).

Light Scattering:

H.C. van de Hulst, "Light Scattering by Small Particles" (John Wiley & Sons, 1957).